PGR5-PGRL1-dependent cyclic electron transport modulates linear electron transport rate in *Arabidopsis thaliana*

Marjaana Suorsa[1†], Fabio Rossi[2†], Luca Tadini[3], Mathias Labs[3], Monica Colombo[4], Peter Jahns[5], Martin M. Kater[2], Dario Leister[3], Giovanni Finazzi[6], Eva-Mari Aro[1], Roberto Barbato[7], Paolo Pesaresi[2*]

[1]Molecular Plant Biology, Department of Biochemistry, University of Turku, FIN-20014 Turku, Finland

[2]Dipartimento di Bioscienze, Università degli studi di Milano, I-20133 Milano, Italy

[3]Plant Molecular Biology (Botany), Department Biology I, Ludwig-Maximilians-Universität München, D-82152 Planegg-Martinsried, Germany

[4]Centro Ricerca e Innovazione, Fondazione Edmund Mach, I-38010, San Michele all'Adige, Italy

[5]Plant Biochemistry, Heinrich-Heine-University Düsseldorf, Universitätsstrasse 1, D-40225 Düsseldorf, Germany

[6]Laboratoire de Physiologie Cellulaire & Végétale, Unité Mixte de Recherche 5168, Centre National de la Recherche Scientifique, Grenoble, France

[7]Dipartimento di Scienze dell'Ambiente e della Vita, Università del Piemonte Orientale, viale Teresa Michel 11, I-15121 Alessandria, Italy

Running title: CET and LET cooperation prevents photoinhibition

* Corresponding author: paolo.pesaresi@unimi.it

† The two authors contributed equally to the manuscript

Pages: 36

Abstract

Plants need a tight regulation of photosynthetic electron transport for survival and growth under environmental and metabolic conditions. For this purpose, the linear electron transport (LET) pathway is supplemented by a number of alternative electron transfer pathways and valves.

In Arabidopsis, cyclic electron transport (CET) around photosystem I (PSI), which recycles electrons from ferrodoxin (Fd) to plastoquinone (PQ), is the most investigated alternative route. However, the interdependence of LET and CET and the relative importance of CET remain unclear, largely due to the difficulty in assessing precisely the contribution of CET in the presence of LET, which dominates electron flow under physiological conditions. We therefore generated Arabidopsis mutants with a minimal water-splitting activity, and thus a low rate of LET, by combining knock-out mutations in *PsbO1*, *PsbP2*, *PsbQ1*, *PsbQ2* and *PsbR* loci. The resulting D5 mutant is viable, although mature leaves contain only ~20% of WT naturally less abundant PsbO2 protein. D5 plants compensate for the reduction in LET by increasing rates of CET, and inducing a strong NPQ response during dark-to-light transitions. To identify the molecular origin of such a high capacity CET, we constructed three sextuple mutants lacking the qE component of NPQ (D5 *npq4-1*), NDH-mediated CET (D5 *crr4-3*) or PGR5-PGRL1-mediated CET (D5 *pgr5*). Their analysis revealed that PGR5-PGRL1-mediated CET plays a major role in DpH formation and induction of NPQ in C3 plants. Moreover, D5 *pgr5* grows under fluctuating light conditions (while *pgr5* dies at the seedling stage), which underlines the importance of PGR5 in modulating intersystem electron transfer.

Introduction

In oxygenic photosynthesis, photosystem II (PSII) – a large pigment-protein complex found in the thylakoid membranes of plants, algae and cyanobacteria – oxidises water molecules and delivers electrons to the plastoquinone (PQ) pool. Besides the PSII core complex associated with the Mn_4O_5Ca cluster, plants and green algae require four additional, lumen-exposed extrinsic proteins – PsbO, PsbP, PsbQ and PsbR – for optimal water oxidation. These proteins, together with the Mn_4O_5Ca cluster, form the so-called oxygen-evolving complex (OEC). In *Arabidopsis thaliana* two isoforms each of PsbO (PsbO1 and PsbO2), PsbP (PsbP1 and PsbP2) and PsbQ (PsbQ1 and PsbQ2) exist, whereas PsbR is encoded by a single-copy gene (Bricker and Frankel 2011, Bricker *et al.* 2012, Ifuku *et al.* 2010, Suorsa *et al.* 2006). Absence of both PsbO isoforms and PsbP1 leads to seedling lethality (Allahverdiyeva *et al.* 2013, Yi *et al.* 2005), whereas plants lacking PsbQ and PsbR show a WT-like phenotype with respect to rates of growth and biomass accumulation under optimal greenhouse conditions (Allahverdiyeva, *et al.* 2013).

Electrons from the PQ pool are transferred via the intersystem electron transfer pathway to photosystem I (PSI), and re-excitation of electrons results in generation of NADPH on the reducing side of PSI. Thus in linear (PSII->PSI) electron transport (LET), both PSII-mediated water splitting and electron flow via the Q-cycle in the Cyt b_6f complex pump protons into the lumen, generating a trans-thylakoid pH gradient (ΔpH) which is used to drive ATP synthesis.

Cyclic electron transfer around PSI (CET) also contributes to ΔpH and ATP formation – without accumulation of NADPH or production of oxygen – with electrons from ferredoxin (Fd) being reinjected into the thylakoid PQ pool (Johnson 2011, Leister and Shikanai 2013, Shikanai 2014, Wang *et al.* 2014).

In Arabidopsis, genetic analyses have provided evidence for two independent routes of CET – one requires a multiprotein complex termed the NADH dehydrogenase-like or NDH complex (Endo *et al.* 1997, Ifuku *et al.* 2011a, Peng *et al.* 2011) and the other a complex involving at least two proteins, PGR5 (Proton Gradient Regulation 5) and PGRL1 (PGR5-Like Photosynthetic Phenotype 1) (DalCorso *et al.* 2008, Hertle *et al.* 2013, Munekage *et al.* 2002).

The NDH complex resembles Complex I in the mitochondrial respiratory chain and mediates electron transport from Fd to PQ (Ogawa and Mi 2007, Yamamoto *et al.* 2011). In Arabidopsis, chloroplast NDH consists of more than 30 subunits which are encoded by both nuclear and organellar genomes, and Arabidopsis NDH constitutively associates with PSI to form a supercomplex (PSI-NDH), that is important to stabilise NDH, especially under high light intensities (Ifuku, *et al.* 2011a, Peng, *et al.* 2011). NDH-mediated electron flow has also been reported to be

crucial in bundle sheath cells of several C4 plants, where it responds to the increased demand for ATP associated with of C4 photosynthesis (Johnson 2011, Majeran and van Wijk 2009).

The PGR5-PGRL1 protein complex mediates the second CET circuit, accepting electrons from Fd and reducing the PQ pool, thus acting as an Fd-PQ reductase (FQR; Hertle, *et al.* 2013). PGR5 owes its name to the high chlorophyll fluorescence phenotype at high light intensities shown by the corresponding missense mutant, which destabilizes the protein (Munekage, *et al.* 2002). The excess light energy absorbed by antenna proteins of PSII is dissipated as heat through a PsbS-mediated mechanism, known as the qE component of non-photochemical quenching (NPQ) (Li *et al.* 2000). The photoprotective qE mechanism is activated by low lumenal pH, and the PGR5 protein is needed to acidify the thylakoid lumen (Munekage *et al.* 2004, Munekage, *et al.* 2002). Plants lacking PGRL1 show a perturbation of CET similar to that seen in PGR5-deficient plants. Moreover, co-purification, yeast two-hybrid and split-ubiquitin assays have demonstrated that PGR5 and PGRL1 interact with each other and form a complex together with PSI (DalCorso, *et al.* 2008, Hertle, *et al.* 2013).

The PGR5-PGRL1 branch of CET is thought to be the major CET pathway in C3 plants, as it is required: (i) to supply the ATP needed to maintain the appropriate ATP/NADPH ratio, (ii) to regulate PSII light harvesting by modulating DpH, resulting in PsbS-mediated qE and (iii) to protect PSI from photoinhibition by regulating LET, in particular the Cyt b_6f complex (Johnson 2011, Suorsa *et al.* 2012).

However, the physiological role of PGR5-PGRL1-mediated CET and the precise functions of PGR5 and PGRL1 remain open, primarily due to technical constraints in accurately assaying CET under conditions in which linear electron flow predominates (Leister and Shikanai 2013).

Here, we report the isolation and characterization of a viable Arabidopsis mutant carrying the simplest OEC complex possible. This mutant carries five different mutations (*psbo1-1 psbp2-1 psbq1-1 psbq2-1 psbr-1*) and is hereafter referred to as D5. This genetic strategy was chosen in preference to the application of chemical inhibitors such as 3-(3,4-dichlorophenyl)-1,1-dimethylurea (DCMU), because it i) allows for specific diminution of LET, ii) provides enough material for any kind of *in vivo* analysis, and iii) allows analyses to be conducted on whole plants. In particular, the D5 mutant accumulates only a limited amount of PsbO2 in mature leaves, and is characterised by reduced LET and a marked increase in CET and NPQ during dark-to-light transition. Furthermore, generation and characterization of sextuple mutants additionally devoid of (i) NDH-mediated CET (D5 *crr4-3*), (ii) PGR5-PGRL1-mediated CET (D5 *pgr5*) and (iii) the qE

component of NPQ (Δ5 *npq4-1*, in which PsbS is completely absent), point to a major role of PGR5-PGRL1 CET in the modulation of LET upon rapid changes in light intensities.

Results

PsbO2 and *PsbP1* together provide sufficient OEC activity for plant viability

Knock-out mutations in nuclear genes encoding OEC subunits were combined to obtain viable Arabidopsis plants with significantly diminished PSII water-splitting activity and LET. The *psbq1-1 psbq2-1 psbr-1* triple mutant, which lacks PsbQ and PsbR and displays a wild type (WT)-like phenotype (Allahverdiyeva, *et al.* 2013), was first crossed with plants devoid of PsbO1, which are characterised by slow growth and pale-green leaves (Figure 1 and S1; Allahverdiyeva *et al.* 2009, Murakami *et al.* 2002, Murakami *et al.* 2005). In contrast, the *psbo2-1* mutant was indistinguishable from WT, in terms of growth rate and leaf pigmentation (Figure S1 and Table 1), whereas plants devoid of PsbO2 subunit and heterozygous at the *PsbO1* locus, *psbo2-1 PsbO1/psbo1-1*, showed intermediate growth rate and leaf pigmentation when compared with *psbo* single mutants (Figure S1), indicating that PsbO1 functions in a dose-dependent manner. Furthermore, complete absence of PsbO is incompatible with plant viability, as the *psbo1-1 psbo2-1* double mutant is seedling-lethal (Figure S1; Yi, *et al.* 2005).

Similarly, *psbp1* plants have been reported to grow only on sucrose-supplemented medium (Allahverdiyeva, *et al.* 2013). Therefore the single mutant *psbp2-1*, which has a WT phenotype, was selected to generate the *psbo1-1 psbp2-1 psbq1-1 psbq2-1 psbr-1* (Δ5) quintuple mutant (Figure 1), which expresses the simplest OEC compatible with autotrophic growth.

Interestingly, *psbo1-1* and Δ5 plants were almost indistinguishable when grown under optimal greenhouse conditions, exhibiting the same pale green color (Table 1) and virtually identical growth rates.

To investigate the consequences of a lack of CET in plants with reduced PSII activity, *psbo1-1* and Δ5 plants were further crossed with *pgr5* and *crr4-3* to generate the corresponding double (*psbo1-1 pgr5*, *psbo1-1 crr4-3*) and sextuple (Δ5 *pgr5*, Δ5 *crr4-3*) mutants. Furthermore, to evaluate the physiological importance of PGR5-PGRL1 CET above and beyond its role in NPQ induction, *psbo1-1* and Δ5 plants were also crossed with *npq4-1* to generate *psbo1-1 npq4-1* and Δ5 *npq4-1* mutants (Figure 1).

When grown under controlled growth-chamber conditions (see also Methods), all double and sextuple OEC mutants, with one exception (Δ5 *npq4-1*), showed a visible phenotype similar to

that of *psbo1-1* and D5 plants, whereas D5 *npq4-1* was characterised by higher growth rate and darker-green coloration of leaves than the quintuple mutant (see also Table 1).

Altered OEC composition has an impact on thylakoid proteins and the organization of thylakoid protein complexes

OEC protein composition was investigated by immunoblot analysis of *psbo1-1*, *psbo2-1*, *psbo2-1 PsbO1/psbo1-1* and D5 plants (Figure 2A). All mutants were characterised by the complete loss of one or other of the PsbO isoforms – which are electrophoretically distinguishable, with PsbO1 showing lower mobility than PsbO2 (Lundin *et al.* 2007). Concomitantly, all other OEC subunits were underrepresented in *psbo1-1* and *psbo2-1 PsbO1/psbo1-1* plants, whereas in *psbo2-1* thylakoids only PsbP was affected. Despite the marked phenotypic differences observed between *psbo1-1* and *psbo2-1 PsbO1/psbo1-1* mutant plants (Figure S1), PsbO isoforms accumulated to comparable levels in both, supporting the notion that PsbO2 subunit is intrinsically less active than PsbO1 *in vivo* under optimal growth conditions (Murakami, *et al.* 2005). In particular, the exclusive presence of the O2 isoform in the OEC complex of *psbo1-1* plants is apparently associated with lower levels of PsbQ and PsbR, which probably reflects differences in binding affinity between the mature PsbO isoforms (Figure S2; Murakami, *et al.* 2002, Murakami, *et al.* 2005).

As expected, the D5 OEC complex from 4-week-old (8-leaf rosette stage) plants was made up of PsbO2 only (21% of WT level), since the simultaneous absence of PsbQ and PsbR subunits led to the disappearance of PsbP1, in agreement with previous findings (Allahverdiyeva, *et al.* 2013).

To monitor the effects of altered OEC subunit composition on the thylakoid electron transport chain (ETC), levels of the major thylakoid protein complex subunits were also investigated in WT, *psbo* single mutants and D5 plants (Figure 2B and C). A general drop in PSII core (D1, D2, CP47) and PSI core (PsaA, PsaD and PsaF) subunits (Figure 2B), and antenna proteins (Figure 2C) coupled with PSI (Lhca2, Lhca3, Lhca4) and PSII (Lhcb3, Lhcb4, Lhcb5), was observed in *psbo1-1* and D5 leaves. Interestingly, effects on PSI and PSII proteins, with the only exception of PSII-D2, were more pronounced in *psbo1-1* than in quintuple mutant thylakoids, and the abundance of Cyt b_6f (PetB and PetC) subunits was actually higher in the thylakoids of D5 plants than in WT. In contrast to *psbo1-1* and D5 plants, accumulation of PSI, LHCI, Cyt b_6/f and ATP synthase subunits in the *psbo2-1* mutant was quite WT-like, whereas PSII core and antenna proteins were slightly down-regulated. As expected, the reductions in thylakoid protein accumulation were accompanied by lower total chlorophyll contents in both *psbo1-1* and D5 leaves (Table 1).

The abundances of key thylakoid regulatory proteins, including PsbS (Li, *et al.* 2000), the kinases STN7 and STN8 and phosphatases TAP38/PPH1 and PBCP required for PSII antenna and PSII

core (de)phosphorylation, respectively (Bellafiore *et al.* 2005, Bonardi *et al.* 2005, Pribil *et al.* 2010, Samol *et al.* 2012, Shapiguzov *et al.* 2010), PGRL1, the L subunit of the NDH complex (NdhL; Shimizu *et al.* 2008) and the Plastid Terminal Oxidase (PTOX) involved in chlororespiration (Carol *et al.* 1999), were also monitored (Figure 2D). The TAP38/PPH1 and PBCP phosphatases responded in opposite ways: the level of TAP38/PPH1 fell by about 40 % while that of PBCP increased by ~twofold in *psbo1-1* and D5 leaves. PTOX also accumulated to higher levels in *psbo1-1* and D5, whereas the abundance of all other regulatory proteins was unaltered in mutant thylakoids.

Immunoblot analyses were also performed on D5 *pgr5*, D5 *crr4-3* and D5 *npq4-1* sextuple mutants to verify the absence of proteins involved in CET (PGR5, PGRL1, NdhL) and NPQ (PsbS). As expected, PGR5, NdhL and PsbS proteins were totally absent in the corresponding sextuple mutants, and there was a marked decrease in PGRL1 levels in plants devoid of PGR5 (Figure 2E).

We next looked at changes in PSII and PSI supercomplex organization. Thylakoid membranes from WT, single and multiple mutants were solubilized with β-dodecyl maltoside or digitonin, and analysed by large-pore Blue Native PAGE in the first dimension (Figure 3A and 3B, Figure S3A and S3B) and by SDS-PAGE in the second (Figure 3C and 3D and Figure S3C and S3D). In samples solubilised with β-dodecyl maltoside, prominent reductions in PSII-LHCII supercomplexes (PSII-LHCIIsc) were observed in D5 and, to a lesser extent, in *psbo1-1* and *psbo2-1 PsbO1/psbo1-1* thylakoids (Figure 3A and 3C and Figure S3A and S3C). The absence of either CET or NPQ subunits had no further impact on these complexes in the corresponding double and sextuple mutants. However, no PSI-NDH megacomplexes (PSI-NDHmc) were detectable in *crr4-3*, *psbo1-1 crr4-3* or D5 *crr4-3* plants.

Digitonin-solubilised thylakoid membranes (Figure 3B and 3D and Figure S3B and S3D), which mainly comprise non-appressed thylakoid domains, also revealed differences in levels of the PSI-LHCI-LHCII protein complex, which was underrepresented in all OEC mutants with the exception of *psbo2-1*. As this protein complex reflects the migration of phosphorylated LHCII from PSII to PSI during state transitions, this finding points to alterations in thylakoid protein phosphorylation (Pesaresi *et al.* 2009).

OEC mutant plants exhibit an unprecedented thylakoid protein phosphorylation pattern

Thylakoid protein phosphorylation is regulated by light conditions and reflects the redox state of the PQ pool and, more generally, of the thylakoid electron carriers downstream of the PQ pool. In order to address thylakoid redox regulation in WT and OEC-defective plants, the phosphorylation status of PSII core (P-D1, P-D2 and P-CP43) and LHCII (P-LHCII) proteins was determined after

acclimation to darkness (D), and exposure to standard growth light (GL) or light selectively exciting either PSI or PSII. In line with earlier data, phosphorylation of almost all PSII core (P-D1, P-D2) and LHCII proteins in WT plants increases under both standard (growth light, GL) and PSII-enriched light conditions (PSII), and decreases in the dark (D) or under light conditions that favour PSI (Figure 4 and S3E). The only exception is P-CP43, which accumulates to higher levels in the dark than in GL-acclimated leaves (see also Fristedt *et al.* 2010). Intriguingly, in *psbo2-1* thylakoids, which are characterised by only a marginal alteration in OEC composition (Figure 2A) and show no deleterious effect on growth rate (Figure S1) or leaf pigment content (Table 1), dephosphorylation of P-D1 and P-D2 under dark conditions is largely abrogated and P-CP43 is maintained at relatively high levels under PSI-favouring light, whereas PSII core protein phosphorylation was similar to WT after exposure to GL- and PSII-enriched light (Figure 4). The altered phosphorylation pattern seen under PSI-enriched light conditions was exacerbated in plants with either a reduced content of PsbO1 (*psbo2-1 PsbO1/psbo1-1*) or devoid of the PsbO1 isoform, as in the case of *psbo1-1*, since the relative phosphorylation of P-CP43, P-D2, P-D1 was markedly higher than in WT plants acclimated to the same light conditions (Figure S3E). On the other hand, a general drop in PSII core phosphorylation was observed in *psbo2-1 PsbO1/psbo1-1* and *psbo1-1* thylakoids, especially under GL- and PSII-enriched light regimes, whereas D5 leaves showed no accumulation of P-D1 and P-D2 in the dark or under the different light conditions, and only a limited amount of P-CP43 accumulated after acclimation to GL- and PSII-enriched light. Furthermore, no P-D1 accumulation was detectable in thylakoids of D5 *pgr5*, D5 *crr4-3* or D5 *npq4-1* sextuple mutants, whereas increased levels of P-D2 and P-CP43 were observed in D5 *pgr5* and D5 *crr4-3* under PSII-enriched, and in D5 *npq4-1* plants under GL- and PSII-enriched light conditions.

OEC-defective mutants were also characterised by a very unusual pattern of LHCII phosphorylation. Indeed, relatively high levels of P-LHCII were observed in nearly all mutants upon acclimation to PSI-enriched light, the only exceptions being D5 *pgr5* and D5 *crr4-3*. This indicates that CET influences LHCII phosphorylation under light conditions that favour PSI activity. Moreover, in thylakoids isolated from dark-acclimated *psbo1-1* and D5 leaves, P-LHCII accumulated to levels higher than in WT, while a marked decrease in P-LHCII was observed in all mutants acclimated to GL- and PSII-enriched light conditions, which reflects the reduced water-spitting activity of PSII.

Arabidopsis plants adapt to OEC defects by rapid and massive induction of PGR5-PsbS-dependent NPQ

To estimate the photochemical efficiency of PSII complexes, chlorophyll *a* fluorescence was monitored in WT and mutant leaves at different actinic light intensities (Figure 5A and Figure S4A) using a Pulse Amplitude Modulated (PAM) fluorimeter. Maximum (F_V/F_M) and effective quantum yields of PSII (Φ_{II}) were markedly reduced in D5 leaves relative to WT (Figure 5A), and somewhat less pronounced effects were observed in both *psbo2-1 PsbO1/psbo1-1* and *psbo1-1* plants, but not in *psbo2-1*, which showed WT-like behaviour (Figure S4A). F_V/F_M and Φ_{II} values were reduced further when the *pgr5* mutation was introduced into either the *psbo1-1* (*psbo1-1 pgr5*) or D5 (D5 *pgr5*) background, whereas the *crr4-3* mutation did not cause any major reduction of PSII activity in either *psbo1-1 crr4-3* or D5 *crr4-3* leaves. On the contrary, the absence of PsbS subunit in *psbo1-1 npq4-1* and D5 *npq4-1* plants resulted in partial rescue of the impaired photosynthetic phenotype, particularly under low and medium actinic light intensities. Furthermore, the redox state of the PQ pool, estimated by measuring the 1-qL parameter at different light intensities (Figure 5B), was higher in D5 *pgr5*, D5 *crr4-3* and D5 *npq4-1* than D5 leaves at low light intensities (less than 200 µmol photons m^{-2} sec^{-1}), whereas 1-qL values were almost indistinguishable at higher light regimes.
In agreement with the data on PSI-LHCI-LHCII complex levels and LHCII phosphorylation, D5, D5 *pgr5*, *D5 crr4-3* and D5 *npq4-1* leaves failed to display state transitions, estimated by measuring the qT parameter, 77 K fluorescence emission spectra and the phosphorylation pattern of LHCII under PSI- and PSII-specific lights (Figure 6). The same measurements highlighted defects in energy redistribution between the two photosystems in *psbo1-1* and in the double mutants *psbo1-1 pgr5*, *psbo1-1 crr4-3* and *psbo1-1 npq4-1*, but not in *psbo2-1* plants (Figure S5).
Measurements of the steady-state levels of non-photochemical quenching under low light conditions (6 µmol photons m^{-2} sec^{-1}) revealed an almost eightfold increase in D5 plants (NPQ, 0.46) with respect to WT (NPQ, 0.06). Higher levels of NPQ were maintained up to a light intensity of 22 µmol photons m^{-2} sec^{-1}, whereas values lower than WT were observed at light intensities higher than 100 µmol photons m^{-2} sec^{-1} (Figure 5C). In particular, at the highest light intensity used in the experiment (825 µmol photons m^{-2} sec^{-1}), NPQ levels decreased by almost 80 % in D5 leaves (0.40 *vs* 1.67 of WT), indicating reduced electron flow and proton gradient formation across the mutant thylakoid membranes. Identical steady-state NPQ behavior was observed in D5 *crr4-3* leaves, whereas NPQ was almost abolished in D5 *pgr5* and D5 *npq4-1* at all actinic light intensities tested.
Steady-state NPQ levels in *psbo2-1 PsbO1/psbo1-1* and *psbo1-1* plants (Figure S4B) were also two-fold higher than in WT or the *psbo2-1* single mutant at low light intensities (6 µmol photons m^{-2} sec^{-1}), and decreased to about 50% of WT level at 825 µmol photons m^{-2} sec^{-1}. Again, *pgr5* and

npq4-1 mutations abolished NPQ in *psbo1-1 pgr5* and *psbo1-1 npq4-1* double mutants, respectively, but *crr4-3* had no effect, as observed in *psbo1-1 crr4-3* leaves.

To investigate further the behaviour of NPQ in WT and mutant plants, the induction of transient NPQ was monitored during the dark-to-light transition (Finazzi *et al.* 2004, Munekage, *et al.* 2002). NPQ was transiently induced within 1 min of exposure to light (53 µmol photons m^{-2} sec^{-1}) in WT leaves, and relaxed within 2 min after the onset of illumination (Figure 5D). Both D5 and D5 *crr4-3* mutants exhibited much higher levels of NPQ than WT during the rapid and transient induction, which also took place within about 1 min, and the relaxation phase was completed within 3 min. In contrast, rapid NPQ induction was virtually absent in D5 *pgr5* and undetectable in D5 *npq4-1* plants. Similarly, *psbo2-1 PsbO1/psbo1-1*, *psbo1-1* and *psbo1-1 crr4-3* showed slightly faster induction and attained higher NPQ values than WT after 1 min of illumination (Figure S4C). Again, NPQ induction was markedly reduced in *psbo1-1 pgr5* and abolished in *psbo1-1 npq4-1*, essentially reproducing the induction and relaxation kinetics of *pgr5* and *npq4-1* single mutants, respectively.

A further approach, based on fluorescence imaging at room temperature (see Methods), was employed to monitor the kinetics of NPQ induction during the transition from darkness to illumination at rates of either 90 or 600 µmol photons m^{-2} sec^{-1} (Figure 7).

In agreement with PAM-derived data, faster and more pronounced induction of NPQ, relative to WT, was observed within 1 min of illumination (90 µmol photons m^{-2} sec^{-1}) in D5 and D5 *crr4-3* leaves (Figure 7A). After 2 min of illumination, D5 and D5 *crr4-3* NPQ levels were lower than in WT and showed a reduction of about 50% by the end of the illumination period (10 min). As expected, PGR5 and PsbS proteins are mainly responsible for rapid (within 1 min of illumination) NPQ induction, as shown by its marked reduction in D5 *pgr5* and its absence in D5 *npq4-1* plants.

The transition from dark to 600 µmol photons m^{-2} sec^{-1} revealed a similar trend in NPQ induction kinetics, although differences between D5 and D5 *crr4-3* on the one hand, and WT and the rest of the mutants on the other, were much more pronounced (Figure 7B). In particular, D5 and D5 *crr4-3* leaves reached their maximum levels of NPQ (2.73 and 2.32, respectively) after 1.5 min of illumination, whereas in WT NPQ increased continuously over 10 min of illumination, to reach a maximum value of 1.95. In contrast, in D5 *pgr5* NPQ induction was very limited and the maximum value (1.38) was reached after 0.6 min of illumination, whereas D5 *npq4-1* leaves did not show any rapid induction of NPQ during the dark-to-light transition. At the end of the illumination period, all mutant plants showed an almost four-fold reduction in NPQ with respect to WT. Estimation of the proton conductivity of the thylakoid ATPase (g_{H^+}) was also conducted to verify the existence of a correlation between the different NPQ induction kinetics and the ATPase activity (Figure 7C).

However, WT and mutant plants showed comparable g_{H^+} values, with the only exception of *pgr5* leaves characterised by an almost two-fold increase with respect to WT g_{H^+} levels (see also Avenson et al., 2005; Suorsa et al., 2012), indicating that ATP synthase conductivity could not account for the observed differences in NPQ induction kinetics and steady-state levels.

PGR5 controls thylakoid electron flow

The overall function of the photosynthetic ETC, including changes in LET and CET, was also evaluated by measuring the ElectroChromic Shift (ECS) spectral changes in WT and mutant leaves (Figure 8A). Linear electron transport (LET), i.e. the rate of PSI and PSII photochemistry, was evaluated from the differences (S_L-S_D) between the slopes of the ECS signal immediately before (S_L) and after (S_D) the red light (120 sec of illumination) was switched off (for further details see Methods). Illumination with far-red light for 120 sec markedly decreases PSII turnover, making the S_L and S_D slopes directly proportional to PSI activity, and thus reflecting the rate of CET. Interestingly, the CET/(CET+LET) ratio after 120 sec of illumination was 1.54- and 1.68-fold higher in D5 (0.097 ± 0.014) and D5 *crr4-3* (0.106 ± 0.011), respectively, than the WT leaves (0.063 ± 0.016), whereas *crr4-3* (0.068 ± 0.017) and *npq4-1* (0.058 ± 0.010) plants showed values comparable to WT. A ratio higher than WT was also observed in D5 *npq4-1* plants (0.099 ± 0.026), whereas D5 *pgr5* (0.038 ± 0.013) and *pgr5* (0.031 ± 0.005) plants showed a reduction of about 40-50% with respect to WT and 60% relative to D5 leaves, indicating that the PGR5-PGRL1-dependent CET is highly active in plants with the minimal OEC protein complex. A similar trend was also observed when CET was monitored in ruptured chloroplasts as an increase in chlorophyll fluorescence after the addition of Fd and NADPH under low measuring light (Munekage et al., 2002; Figure 8B). In *pgr5* as in D5 *pgr5*, the increase in chlorophyll fluorescence reached a markedly lower plateau compared to WT. In the same assay D5, D5 *crr4-3* and D5 *npq4-1* exhibited an increased CET efficiency compared to WT, as indicated by the fact that chlorophyll fluorescence reached a higher plateau, thus confirming that PGR5-PGRL1-dependent CET is highly active in plants with the minimal OEC protein complex.Indeed, PGR5 is so crucial for the regulation of intersystem electron transport that the *pgr5* mutant died at the seedling stage when grown under fluctuating light conditions (Figure 9), whereas fluctuating light conditions had no impact on plants devoid of NDH-dependent CET (*crr4-3* and D5 *crr4-3*) or NPQ (*npq4-1* and D5 *npq4-1*). Importantly, the minimal OEC rescues the lethal phenotype of *pgr5* plants, as shown by the viability of D5 *pgr5* plants grown under fluctuating light conditions (Figure 9).

In agreement with previous reports, the lethality of *pgr5* plants under fluctuating light conditions can be attributed to the permanent reduction of P700 even at low and moderate constant light

intensities [Y(ND) and Y(NA), (Figure 10)]. In fact, the viable D5 *pgr5* plants were capable of oxidizing P700 during the light phase, both under varying and constant light intensities, at levels comparable to those of WT, D5 and the other single and multiple mutants tested (Figure 10). This finding points to a role for the PGR5 protein in the modulation of thylakoid electron flow under fluctuating light levels.

Discussion

The basic operation of LET – electron flow from water to ferredoxin-FNR-NADP via two photosynthetic reaction centres linked in series – is well understood. However, other electron transfer routes are used for particular purposes. The best studied of these in plants is CET around PSI. CET was discovered over 60 years ago (Arnon *et al.* 1954), but some aspects of the process remain elusive, mainly because LET dominates electron flow under most conditions. To gain a better understanding of the physiological role of CET, we employed a genetic strategy to reduce the water-splitting activity of PSII in Arabidopsis to the lowest level compatible with plant viability, consequently decreasing the rate of LET to the minimum required for survival. The resulting mutant, D5, expresses only 21% of the WT level of PsbO2 and lacks all other subunits of the OEC. These plants show a general reorganization of the photosynthetic apparatus, in terms of thylakoid protein composition, supercomplex organization and thylakoid protein phosphorylation. In addition, D5 thylakoids react to the reduced rate of LET by increasing rates of PGR5-PGRL1-dependent CET and rapidly inducing NPQ during dark-to-light transitions, independently of PSII function. Finally, , the ability of D5 *pgr5* plants to oxidize P700 and grow under fluctuating light – unlike the *pgr5* single mutant, which dies at the seedling stage – support a role for PGR5-PGRL1 complexes in modulating thylakoid intersystem electron transport (see Table 2 for a summary of the mutants and their characteristics).

Residual levels of PsbO2 are sufficient for water-splitting activity and plant viability

Recent *in silico* analysis of PsbO sequences in various evolutionarily divergent species have revealed that most angiosperms possesses two isoforms (Duchoslav and Fischer 2015). However, ancient duplications and subsequent neofunctionalization of the isoforms have occurred independently in each angiosperm family, i.e. protein sequences of the paralogues in certain species are more closely related to each other than are isoforms from other species. This indicates that the presence of two PsbO isoforms is likely to provide plants with a greater capacity for environmental acclimation (Duchoslav and Fischer 2015). Furthermore, biochemical studies on eukaryotic PSIIs from spinach and Arabidopsis support the notion that two PsbO subunits are bound per PSII reaction centre (Popelkova *et al.* 2008, Xu and Bricker 1992).

In Arabidopsis, the absence of both PsbO isoforms in *psbo1-1 psbo2-1* plants destabilises the Mn_4O_5Ca cluster and disrupts O_2 production, leading to albino cotyledons and seedling lethality (see Figure S1 and Yi, *et al.* 2005). This finding, together with the observation of an inverse relationship between the amount of PsbO and the severity of the mutant phenotype (compare *psbo2-1* and *pbo1-1* plants, Figure S1), identifies PsbO1 as the major isoform of the OEC, and confirms

that both isoforms are able to stabilise the Mn_4O_5Ca cluster (Allahverdiyeva, *et al.* 2009, Enami *et al.* 2008, Murakami, *et al.* 2005, Shutova *et al.* 2005).

Nevertheless, the two isoforms differ functionally, as shown by the phenotypes and PSII efficiencies of *psbo2-1/PsbO1 psbo1-1* and *psbo1-1* plants, which contain equal amounts of PsbO1 and PsbO2, respectively (see Figure 2A). Immunoblot analyses, together with data on growth rate and photosynthetic performance, indicate that PsbO1 has a higher affinity for PsbQ and PsbR, which would largely account for this difference. The isoforms differ at 11 positions, but only four substitutions are non-conservative (see Figure S2), and previous analyses suggest that Val186Ser, Leu246Ile and Val204Ile suffice to explain the functional inferiority of PsbO2 to PsbO1 (Murakami, *et al.* 2005).

In agreement with previous results, immunoblot analyses confirmed that the PsbO subunit(s) serve(s) to bind the other OEC subunits to PSII, and that PsbP1 plays a role in PSII and OEC assembly, rather than being a component of the PSII-OEC complex (Allahverdiyeva, *et al.* 2013). Moreover, reduced accumulation of PSII-LHCII subunits in the *psbo1-1* and D5 mutants leads to a readjustment of PSI-PSII stoichiometry, as shown by the concomitant decrease in levels of PsaA, PsaD and PsaF, which was more pronounced in *psbo1-1* than in D5 leaves. This finding, and the fact that Cyt b_6f subunits accumulate to higher than WT levels in D5 plants – with no reduction in PGRL1, NDH or PTOX subunit abundance – suggest that plants respond to the changes in OEC composition and LET rate by increasing their usage of alternative electron transport routes (Johnson 2011, McDonald *et al.* 2011). Interestingly, the differential accumulation of the phosphatases TAP38/PPH1 and PBCP in *psbo1-1* and in D5 leaves (Figure 4; see also below) indicates that their activities are controlled via changes in protein accumulation (see also Pribil, *et al.* 2010), as is the case for the cognate kinases STN7 and STN8 (Flood *et al.* 2014, Willig *et al.* 2011, Yin *et al.* 2012). A deficit of TAP38/PPH1 was also observed in Arabidopsis lines carrying the specific amiLHCB1 construct (Pietrzykowska *et al.* 2014), suggesting that TAP38 abundance could be regulated by the level of its substrate Lhcb1.

The architecture of PSII supercomplexes is also influenced by OEC composition. In both *psbo1-1* and D5 thylakoids, amounts of PSII-LHCII and PSI-LHCI-LHCII supercomplexes are severely decreased under growth-chamber light conditions, while levels of unattached LHCII trimers and minor LHCs increase significantly (see Figure 3), in line with earlier reports (Allahverdiyeva, *et al.* 2013, Caffarri *et al.* 2009, Ifuku *et al.* 2011b). Furthermore, these alterations are a direct result of the changes in the OEC complex, as they were unaffected by concomitant downregulation of CET or NPQ (*psbo1-1 pgr5*, *psbo1-1 crr4-3*, *psbo1-1 npq4-1*, D5 *pgr5*, D5 *crr4-3*, and D5 *npq4-1* plants).

OEC mutants show high CET rates during dark-to-light transitions

With the exception of *psbo2-1*, plants with altered OEC composition were characterised by marked reductions in PSII quantum yield, as revealed by chlorophyll fluorescence analysis of *psbo1-1*, *psbo2-1 PsbO1/psbo1-1* and – most strikingly – the D5 mutant, in agreement with reduced water-splitting activity and electron transfer in PSII (see Figure 5 and Figure S4).

Inhibition of the NDH-dependent CET pathway in *psbo1-1* and D5 leaves did not alter the photosynthetic efficiency of *psbo1-1 crr4-3* and D5 *crr4-3* plants, confirming that the contribution of this pathway to thylakoid electron transport in C3 plants is rather modest (Avenson *et al.* 2005, Johnson 2011, Shikanai 2014). In contrast, D5 *pgr5* leaves were characterised by a further impairment of PSII quantum yield which supports a key role of PGR5 in the regulation of the thylakoid electron transport chain.

CET measurements also indicate that plants with a minimal OEC respond to the decrease in LET by raising rates of CET during dark-to-light transitions (see Figure 8). This increase is mediated by the PGR5-PGRL1-dependent pathway, since it is observed in D5 *crr4-3* and D5 *npq4-1*, but not in D5 *pgr5* plants – further supporting a major role for the PGR5-PGRL1-dependent branch of CET in C3 plants (Johnson 2011). PGR5/PGRL1-dependent CET can also control light absorption and thylakoid electron transport by providing a fast and transient mechanism to regulate the level of NPQ, independently of PSII function (Leister and Shikanai 2013, Shikanai 2014). Thus, while *psbo1-1*, D5 and corresponding multiple mutants lacking the NDH-dependent pathway, such as *psbo1-1 crr4-3* and D5 *crr4-3* plants, exhibit a rapid and substantial induction of NPQ during dark-to-light transitions, this response is virtually absent in *psbo1-1 pgr5* and D5 *pgr5* plants, and undetectable in *psbo1-1 npq4-1* and D5 *npq4-1* leaves. Furthermore, the almost identical antenna composition and thylakoid protein super-complex organization (Table 1 and Figure 3), together with the very similar activity of the ATPase (Figure 7C) observed in D5, D5 *crr4-3*, D5 *npq4-1* and D5 *pgr5* leaves, allow to exclude the contribution of other processes in CET rates and NPQ induction kinetics.

PGR5-PGRL1-dependent CET prevents over-reduction of PSI under fluctuating light

Although most OEC mutants have obvious visible phenotypes, none of these was exacerbated by additional defects in either CET or NPQ under optimal growth-chamber conditions. Indeed D5 *npq4-1* plants showed better photosynthetic performance and grew faster than D5, indicating that regulatory mechanisms are superfluous or even deleterious under optimal lighting conditions. This is consonant with a previous report that the Arabidopsis *tap38-1* mutant, which lacks the phosphatase required for state transitions, performed better than WT in terms of photosynthetic

performance and growth rate under optimal growth-chamber conditions (Pribil, *et al.* 2010), and further supports the notion that a comprehensive picture of the physiological importance of photosynthesis regulatory mechanisms can be only obtained by growing mutant plants under varying and stressful conditions.

In agreement with previous findings, the *pgr5* mutant, unlike *crr4-3* and *npq4-1* plants, died at the seedling stage when grown under fluctuating light (Suorsa, *et al.* 2012). This phenotype points to a unique function for PGR5-PGRL1-dependent CET in enabling plant acclimation to fluctuating light (see Figure 9). In particular, the PGR5-PGRL1 complex has been proposed to regulate LET rates under fluctuating light, thus controlling the flux of electrons towards, and preventing photodamage to PSI. The involvement of PGR5 in moderating LET is supported by the fact that the marked reduction of electron transfer from PSII to PSI seen upon introduction of *pgr5* into the D5 backgroundrestores the ability to oxidize P700 (Figure 10) and grow under fluctuating light (Figure 9).

The inability of *pgr5* to induce NPQ does not appear to contribute significantly to PSI photoprotection, since *npq4-1* and D5 *npq4-1* plants show identical phenotypes under constant and fluctuating light conditions,. The same holds for the NDH-dependent CET route, since the response of the *crr4-3* mutant to the different lighting conditions was indistinguishable from that of WT plants,. Nevertheless, D5 *pgr5* plants are clearly impaired in their ability to cope with fluctuating light levels, perhaps because they cannot adjust the ATP/NADPH ratio under stressful conditions. However, this latter point deserves further study, as there is a growing consensus that the chloroplast is not energetically isolated within the cell. Both reducing equivalents and ATP may be transferred directly or indirectly across the chloroplast envelope, in either direction, as determined by metabolic requirements (Johnson 2011).

Changes in usage of electron transfer routes determine thylakoid phosphorylation patterns

The phosphorylation status of the light-harvesting and core proteins of photosystem II is mainly determined by two complementary kinase-phosphatase pairs, STN7/TAP38(PPH1) and STN8/PBCP, respectively (Pesaresi *et al.* 2011, Rochaix *et al.* 2012, Tikkanen and Aro 2012). In plants, the activity of the two kinases is primarily regulated by the redox state of the PQ pool, which in turn depends on the light irradiance and acts as a sensor to reconfigure the allocation of light energy to the two photosystems (Bonardi, *et al.* 2005, Pesaresi, *et al.* 2009).

In D5 plants, the phosphorylation state of PSII core proteins (D1, D2 and, to some extent, CP43) was directly linked to reduced activity of the water-splitting complex and the decreased transfer of electrons into the thylakoid ETC (see Figure 4) rather than the biochemical organization

of the photosynthetic complexes. Indeed, phosphorylation of D1 and D2 proteins was undetectable in D5 plants (i.e. with only 21% of WT PsbO2 levels), irrespective of lighting conditions, even though levels of these proteins were not dramatically altered. The increased accumulation of PBCP cannot explain the decrease in phosphorylation in D5 leaves, since the former is also seen in *psbo1-1* thylakoids, in which PSII core phosphorylation remains close to WT levels. D1 phosphorylation was also undetectable in D5 *pgr5*, D5 *crr4-3* and D5 *npq4-1* leaves, and very low levels of D2 phosphorylation were observed under GL and PSII light in these same mutants, indicating that D1 and D2 phosphorylation is largely independent of PGR5 in plants with a minimal OEC. The link between changes in electron flow and protein phosphorylation patterns was confirmed by the finding that mutants devoid of CET, such as D5 *pgr5* and D5 *crr4-3*, exhibit higher levels of CP43 phosphorylation under PSII-enriched light than D5 plants do, in agreement with the increased reduction of PQ pool (1-qL parameter, Figure 5B). Indeed, comparable levels of CP43 phosphorylation were seen, under both GL and PSII light, in D5 *npq4-1* leaves, which show no NPQ activity.

More importantly, the level of LHCII phosphorylation seen in D5 leaves exposed to different quantities and qualities of light was found to be high in the dark and under PSI-enriched light, absent under GL conditions and very low under PSII light. This pattern is exactly the opposite of that observed in WT plants.

In principle, this phenotype could be explained by reduced TAP38/PPH1 activity, as the phosphatase is much less abundant in D5 thylakoids. But this hypothesis is inconsistent with the finding that dephosphorylation of LHCII takes place in D5 leaves under GL and PSII-enriched light. Moreover, *psbo1-1* thylakoids, which contain as much TAP38/PPH1 as D5 leaves, are characterised by an LHCII phosphorylation pattern similar to that of *psbo2-1*, although TAP38/PPH1 levels in *psbo2-1* thylakoids are comparable to those in WT (see Figures 2 and 4). Therefore we propose that this unique phosphorylation pattern reflects changes in the redox state of the photosynthetic chain arising from differences in electron flow, rather than changes in the relative amounts of the target proteins involved in these phenomena.

In the context of the ”classical” model for state transitions, where, in order to guarantee optimal energy distribution between the two photosystems, the absorption cross-sections of PSII and PSI are regulated in response to light excitation pressure by reversible phosphorylation of LHCII (Rochaix, *et al.* 2012), the LHCII phosphorylation pattern in D5 plants would indicate that mutant leaves are in state-1 under GL- and PSII-enriched light, which favour PSII in the WT, and in state-2 under dark- and PSI-enriched light conditions where PSI activity is normally stimulated.

This apparent contradiction can be rationalized when one considers that the relatively high WT level of phosphorylation of LHCII under PSI-enriched light is drastically reduced in Δ5 *pgr5* and Δ5 *crr4-3*, but not in Δ5 *npq4-1*. This suggests that changes in the balance between CET around PSI and LET enable the STN7 kinase to phosphorylate LHCII under conditions where LET is diminished by PSII impairment. The postulated increase in CET rate in OEC mutants acclimated to PSI-enriched light conditions is also supported by the high level of PSII-LHCII phosphorylation observed in *psbo1-1*, *psbo2-1* and *psbo2-1 PsbO1/psbo1-1* plants under PSI-enriched light.
In agreement with previous data (Hou *et al.* 2003), thylakoid protein phosphorylation is not only regulated by the quality and intensity of light, but is clearly influenced by other factors – including the metabolic (redox) state of the chloroplast – via a shift between LET and CET. In agreement with this idea, the high P-LHCII levels observed in Δ5 thylakoids in the dark are also seen in *psbo1-1*.

Based on these observations, thylakoid protein phosphorylation and PGR5 expression appear to be closely interconnected in higher plants, both to maintain the redox poise of the PQ pool and to respond to metabolic needs. It is also important to note that both CET routes modulate the redox state of the ETC under conditions that favour PSI activity. This probably explains the exacerbated phenotype observed by Munekage et al. (2004) in the *pgr5 crr2* double mutant, which lacks both CET pathways.

Taken together, our data support a major role for PGR5-PGRL1-mediated CET in acclimation to increased light intensities, such as during dark-to-light and low-to-high light transitions. This alternative electron transport pathway is responsible for the rapid generation of the ΔpH across the thylakoid membranes that controls: i) the induction of NPQ, ii) the reoxidation of PSI complexes, and possibly iii) the ATP/NADPH ratio in response to physiological needs. Furthermore, changes in the relative importance of the different electron transport routes have iv) a major impact on the redox regulation of thylakoid protein phosphorylation.

Methods

Plant material and propagation

Arabidopsis thaliana mutant lines in the Columbia-0 (Col-0) background were located in the T-DNA Express Database (http://signal.salk.edu/cgi-bin/tdnaexpress) and obtained from the European Arabidopsis Stock Center. The *psbp2-1*, *psbq1-1*, *psbq2-1* and *psbr-1* alleles have been described previously (Allahverdiyeva, *et al.* 2013). The *psbo1-1* line (Salk_093396), described in Lundin et al. (2008), showed the same phenotype as the *psbo1-2* line (RATM12-1816-1_G) obtained from the RIKEN collection. The *psbo2-1* line (CSHL_ET9214) was obtained from the Cold Spring Harbor Laboratory collection, while *psbo2-2* came from the Salk collection (Alonso *et al.* 2003). Both lines were identical to *psbo2* (Salk_024720) reported in Lundin et al. (2008). The *pgr5* allele is described in Munekage et al. (2002), *crr4-3* in Kotera et al. (2005) and *npq4-1* in Li et al. (2000).

Arabidopsis plants were grown under controlled growth-chamber conditions as described previously (Pesaresi, *et al.* 2009). In experiments with fluctuating light levels, an electronically controlled shading system was used to expose the plants to low light (50 µmol photons m^{-2} sec^{-1}) for 5 min and then to high light (500 µmol photons m^{-2} sec^{-1}) for 1 min (Suorsa, *et al.* 2012) over a photoperiod of 8 h light/16 h dark. In addition, phenotypic analyses were conducted on plants grown on Murashige and Skoog (MS) medium (Duchefa) with or without 1% (w/v) sucrose. Growth measurements are described elsewhere (Leister *et al.* 1999)

Isolation of single and multiple mutants

A. thaliana DNA was isolated as described (Ihnatowicz *et al.* 2004). Lines bearing T-DNA or *Ds* insertions in the nuclear genes encoding OEC subunits, as well as deletions (*npq4-1*) or single nucleotide changes (*pgr5* and *crr4-3*) were identified by targeted PCR and DNA sequencing, using the primer combinations listed in Table S1. The D5 mutant was obtained by crossing the *psbq1-1 psbq2-1 psbr-1* triple mutant (Allahverdiyeva, *et al.* 2013) with *psbp2-1*, then crossing the F1 with either *psbo1-1* or *psbo1-2* and genotyping the corresponding F2 progenies. D5 plants were also crossed with *npq4-1*, *pgr5* and *crr4-3* single mutants to obtain the corresponding sextuple mutants.

PAGE and immunoblot analyses

Thylakoid isolation and fractionation were performed as described in Jarvi et al. (2011). Samples of thylakoid membranes corresponding to 8 µg of chlorophyll were solubilized in the presence of either 1% (w/v) β-dodecyl-maltoside (Sigma-Aldrich) or 1% (w/v) digitonin (Calbiochem) and optimal separation of the thylakoid membrane protein complexes was obtained by large-pore Blue-Native (lpBN)-PAGE. For two-dimensional protein fractionation under denaturing conditions (2D

SDS-PAGE), the denatured strips were transferred onto the top of an SDS-PA gel [15% acrylamide (w/v) containing 6 M urea] and subjected to electrophoresis to determine the subunit composition of the complexes. For protein visualization, gels were stained with silver as described previously (Blum *et al.* 1987).

For immunoblot analyses, total proteins were prepared as described by Martinez-Garcia et al. (1999). Total proteins were fractionated by SDS-PAGE [12% acrylamide (w/v); (Schagger and Vonjagow 1987)]. Proteins were then transferred to polyvinylidene difluoride (PVDF) membranes (Ihnatowicz, *et al.* 2004) and replicate filters were immunodecorated with antibodies specific for OEC protein complex (PsbO, PsbP, PsbQ), PSI (PsaA, PsaD, PsaF) and PSII (D1, D2, CP47) core proteins, PSI (Lhca2, Lhca3, Lhca4) and PSII (Lhcb3, Lhcb4, Lhcb5) antenna proteins, Cyt b_6f (PetB and PetC), plastocyanin (PetE), all obtained from Agrisera (http://www.agrisera.com/en/artiklar/plantalgal-cell-biology/index.html). The PGR5-specific Ab was obtained from Toshiharu Shikanai's lab, whereas PGRL1, NdhL, STN7, STN8, TAP38 and PsbS Abs were provided by Roberto Barbato. The PBCP Ab was kindly provided by Michel Goldschmidt-Clermont's lab.

For phosphorylation analyses, thylakoids were isolated from WT and mutant plants kept overnight in the dark, or exposed to growth light (100 µmol photons m^{-2} s^{-1}), or to PSI- or PSII-enriched light as described in Tikkanen et al. (2006). Thylakoids were isolated as described above, fractionated by SDS-PAGE, transferred to PVDF membrane and immunolabelled with a polyclonal anti-phosphothreonine antibody (New England BioLabs, Beverly, MA, http://www.neb.com/nebecomm/default.asp).

Chlorophyll *a* fluorescence and pigment analyses

In vivo Chl *a* fluorescence of leaves was measured using the Dual-PAM-100 (Walz, http://www.walz.com/) as described previously (Pesaresi, *et al.* 2009), and the parameters F_V/F_M, Φ_{II} (Genty *et al.* 1989), 1-qL and steady-state NPQ (Grasses *et al.* 2002) were quantified. The time-course of induction and relaxation of NPQ during dark-to-light transitions was measured on dark-adapted plants exposed to light (53 µmol photons m^{-2} sec^{-1}) for 4 min followed by 2 min of dark, as described in DalCorso et al. (2008). Quenching of chlorophyll fluorescence due to state transitions (qT) was determined by illuminating dark-adapted leaves with blue light (35 µmol m^{-2} s^{-1}, 10 min) and then measuring the maximum fluorescence in state 2 (Fm2). Next, state 1 was induced by superimposing far-red light (255 µmol m^{-2} s^{-1}, 10 min) and recording Fm1. qT was calculated as (Fm1-Fm2)/Fm2 (Jensen *et al.* 2000).

The Dual-PAM-100 was also employed to monitor variations in PSI donor-side [Y(ND)] and acceptor-side [Y(NA)] limitations, by measuring the redox state of P700 at room temperature under different light intensities. Alternatively, fluorescence transients were imaged using a Speedzen MX fluorescence imaging setup (JBeamBio, France) as described (Allorent *et al.* 2013). NPQ was calculated as $(F_m-F_m')/F_m'$, where F_m and F_m' are, respectively, the maximum levels of fluorescence emission measured in the dark and upon light exposure (90 and 600 µmol photons m^{-2} sec^{-1}) for 10 min followed by 10 min dark. Intact plants were imaged and mean values for 15 leaves were calculated for each light intensity.

State transitions were also assessed by 77 K fluorescence measurements. Chlorophyll a fluorescence emission spectra were obtained from frozen suspension at 77 K by using an Ocean Optics QE Pro Spectrometer. Thylakoid membranes isolated from leaves adapted for 1 hour to state 1 light (far red light: 30 µmol photons m^{-2} s^{-1}) and state 2 light (red light: 50 µmol photons m^{-2} s^{-1}) were diluted to 1 µg of Chl mL^{-1} in storage buffer containing 100 mm sorbitol, 50 mm HEPES (pH 7.5), 10 mm NaF, and 10 mm MgCl2 and excited at 475 nm. The raw spectra were normalized at 685 nm for comparison of florescence emission bands from PSI.

In vivo spectroscopic measurements were performed with a JTS 10 spectrophotometer (BioLogic, France). Changes in linear (LET) and cyclic (CET) electron flow were evaluated by measuring the Electrochromic Shift (ECS) signal, a shift in the pigment absorption bands that is linearly correlated with the number of light-induced charge separations within the reaction centers (Bailleul *et al.* 2010). LET and CET were calculated from the relaxation kinetics of the ECS signal in the dark (Joliot and Joliot 2002, Sacksteder *et al.* 2000). In brief, the ECS signal measured under steady-state illumination results from concomitant transmembrane potential generation by PSII, the cytochrome b_6f complex and PSI and from transmembrane potential dissipation by the ATP synthase CF_0-F_1. When the light is switched off, reaction center activity immediately ceases, while ATPase and the cytochrome b_6f complex activities remain (transiently) unchanged. Therefore, the difference between the slopes of the ECS signal measured in the light [120 sec of red light (600 µmol photons m^{-2} sec^{-1})] and after the light is switched off (S_L-S_D) is proportional to the rate of PSI and PSII photochemistry (i.e. to the rate of "total' electron flow). This can be calculated by dividing (S_L-S_D) by the amplitude of the absorption changes induced by the transfer of one charge across the membrane (e.g. one PSI turnover). The latter is estimated as the amplitude of the ECS signal upon exposure to a saturating single turnover laser flash under conditions where PSII is inactive (see above). The rate of cyclic electron flow can be evaluated using the same approach under far-red light (120 sec of saturating far-red light), where PSII activity is greatly reduced, while PSI activity

is preserved. In this case, the S_L-S_D slope divided by PSI charge separation mainly reflects cyclic electron flow.

Eventually, occurrence of CET activity was also assessed in ruptured chloroplasts as described in Munekage et al. (2002) using 5 µM of spinach ferrodoxin (Sigma) and 0.25 mM NADPH.

Relative estimates of the conductivity of the thylakoid to protons (g_{H^+}), primarly attributable to the turnover of the ATP synthase, were obtained by taking the inverse of the time constant for ECS decay as described in Avenson et al. (2005).

Pigments were analyzed by reverse-phase HPLC (Farber *et al.* 1997).

Acknowledgments

We thank Virpi Paakkarinen and Marjaana Rantala for the excellent technical assistance and Paul Hardy for critical reading of the manuscript. M.S. was supported by Academy of Finland (project nos. 271832 and 273870).

Author contributions

F.R., M.C. and P.P. conceived and conducted the generation and analysis of single and multiple mutants; M.S. conceived and conducted Native (lpBN)-PAGE, and 2D SDS-PAGE; L.T., F.R. and M.S. performed immunoblot analyses; P.J. conducted pigment analysis; G.F., M.L. and P.P. conceived and conducted LET, CET and NPQ measurements; E-M.A., M.K., D.L. R.B. and P.P. designed and conceived the study. P.P. and M.S wrote the manuscript

References

Allahverdiyeva, Y., Mamedov, F., Holmstrom, M., Nurmi, M., Lundin, B., Styring, S., Spetea, C. and Aro, E.M. (2009) Comparison of the electron transport properties of the psbo1 and psbo2 mutants of Arabidopsis thaliana. *Biochim Biophys Acta*, **1787**, 1230-1237.

Allahverdiyeva, Y., Suorsa, M., Rossi, F., Pavesi, A., Kater, M.M., Antonacci, A., Tadini, L., Pribil, M., Schneider, A., Wanner, G., Leister, D., Aro, E.M., Barbato, R. and Pesaresi, P. (2013) Arabidopsis plants lacking PsbQ and PsbR subunits of the oxygen-evolving complex show altered PSII super-complex organization and short-term adaptive mechanisms. *Plant J*, **75**, 671-684.

Allorent, G., Tokutsu, R., Roach, T., Peers, G., Cardol, P., Girard-Bascou, J., Seigneurin-Berny, D., Petroutsos, D., Kuntz, M., Breyton, C.c., Franck, F., Wollman, F.-A., Niyogi, K.K., Krieger-Liszkay, A., Minagawa, J. and Finazzi, G. (2013) A Dual Strategy to Cope with High Light in Chlamydomonas reinhardtii. *The Plant Cell Online*, **25**, 545-557.

Alonso, J.M., Stepanova, A.N., Leisse, T.J., Kim, C.J., Chen, H., Shinn, P., Stevenson, D.K., Zimmerman, J., Barajas, P., Cheuk, R., Gadrinab, C., Heller, C., Jeske, A., Koesema, E., Meyers, C.C., Parker, H., Prednis, L., Ansari, Y., Choy, N., Deen, H., Geralt, M., Hazari, N., Hom, E., Karnes, M., Mulholland, C., Ndubaku, R., Schmidt, I., Guzman, P., Aguilar-Henonin, L., Schmid, M., Weigel, D., Carter, D.E., Marchand, T., Risseeuw, E., Brogden, D., Zeko, A., Crosby, W.L., Berry, C.C. and Ecker, J.R. (2003) Genome-wide insertional mutagenesis of Arabidopsis thaliana. *Science*, **301**, 653-657.

Arnon, D.I., Allen, M.B. and Whatley, F.R. (1954) Photosynthesis by isolated chloroplasts. *Nature*, **174**, 394-396.

Avenson, T.J., Cruz, J.A., Kanazawa, A. and Kramer, D.M. (2005) Regulating the proton budget of higher plant photosynthesis. *Proc Natl Acad Sci U S A*, **102**, 9709-9713.

Bailleul, B., Cardol, P., Breyton, C. and Finazzi, G. (2010) Electrochromism: a useful probe to study algal photosynthesis. *Photosynthesis Research*, **106**, 179-189.

Bellafiore, S., Barneche, F., Peltier, G. and Rochaix, J.D. (2005) State transitions and light adaptation require chloroplast thylakoid protein kinase STN7. *Nature*, **433**, 892-895.

Blum, H., Beier, H. and Gross, H.J. (1987) Improved Silver Staining of Plant-Proteins, Rna and DNA in Polyacrylamide Gels. *Electrophoresis*, **8**, 93-99.

Bonardi, V., Pesaresi, P., Becker, T., Schleiff, E., Wagner, R., Pfannschmidt, T., Jahns, P. and Leister, D. (2005) Photosystem II core phosphorylation and photosynthetic acclimation require two different protein kinases. *Nature*, **437**, 1179-1182.

Bricker, T.M. and Frankel, L.K. (2011) Auxiliary functions of the PsbO, PsbP and PsbQ proteins of higher plant Photosystem II: a critical analysis. *J Photochem Photobiol B*, **104**, 165-178.

Bricker, T.M., Roose, J.L., Fagerlund, R.D., Frankel, L.K. and Eaton-Rye, J.J. (2012) The extrinsic proteins of Photosystem II. *Biochim Biophys Acta*, **1817**, 121-142.

Caffarri, S., Kouril, R., Kereiche, S., Boekema, E.J. and Croce, R. (2009) Functional architecture of higher plant photosystem II supercomplexes. *Embo J*, **28**, 3052-3063.

Carol, P., Stevenson, D., Bisanz, C., Breitenbach, J., Sandmann, G., Mache, R., Coupland, G. and Kuntz, M. (1999) Mutations in the Arabidopsis gene IMMUTANS cause a variegated phenotype by inactivating a chloroplast terminal oxidase associated with phytoene desaturation. *Plant Cell*, **11**, 57-68.

DalCorso, G., Pesaresi, P., Masiero, S., Aseeva, E., Schunemann, D., Finazzi, G., Joliot, P., Barbato, R. and Leister, D. (2008) A complex containing PGRL1 and PGR5 is involved in the switch between linear and cyclic electron flow in Arabidopsis. *Cell*, **132**, 273-285.

Duchoslav, M. and Fischer, L. (2015) Parallel subfunctionalisation of PsbO protein isoforms in angiosperms revealed by phylogenetic analysis and mapping of sequence variability onto protein structure. *BMC Plant Biol*, **15**, 133.

Enami, I., Okumura, A., Nagao, R., Suzuki, T., Iwai, M. and Shen, J.R. (2008) Structures and functions of the extrinsic proteins of photosystem II from different species. *Photosynth Res*, **98**, 349-363.

Endo, T., Mi, H.L., Shikanai, T. and Asada, K. (1997) Donation of electrons to plastoquinone by NAD(P)H dehydrogenase and by ferredoxin-quinone reductase in spinach chloroplasts. *Plant and Cell Physiology*, **38**, 1272-1277.

Farber, A., Young, A.J., Ruban, A.V., Horton, P. and Jahns, P. (1997) Dynamics of Xanthophyll-Cycle Activity in Different Antenna Subcomplexes in the Photosynthetic Membranes of Higher Plants (The Relationship between Zeaxanthin Conversion and Nonphotochemical Fluorescence Quenching). *Plant Physiol*, **115**, 1609-1618.

Finazzi, G., Johnson, G.N., Dall'Osto, L., Joliot, P., Wollman, F.A. and Bassi, R. (2004) A zeaxanthin-independent nonphotochemical quenching mechanism localized in the photosystem II core complex. *Proc Natl Acad Sci U S A*, **101**, 12375-12380.

Flood, P.J., Yin, L., Herdean, A., Harbinson, J., Aarts, M.G. and Spetea, C. (2014) Natural variation in phosphorylation of photosystem II proteins in Arabidopsis thaliana: is it caused by genetic variation in the STN kinases? *Philos Trans R Soc Lond B Biol Sci*, **369**, 20130499.

Fristedt, R., Granath, P. and Vener, A.V. (2010) A protein phosphorylation threshold for functional stacking of plant photosynthetic membranes. *PLoS One*, **5**, e10963.

Genty, B., Briantais, J.M. and Baker, N.R. (1989) The Relationship between the Quantum Yield of Photosynthetic Electron-Transport and Quenching of Chlorophyll Fluorescence. *Biochim Biophys Acta*, **990**, 87-92.

Grasses, T., Pesaresi, P., Schiavon, F., Varotto, C., Salamini, F., Jahns, P. and Leister, D. (2002) The role of Delta pH-dependent dissipation of excitation energy in protecting photosystem II against light-induced damage in Arabidopsis thaliana. *Plant Physiol Bioch*, **40**, 41-49.

Hertle, A.P., Blunder, T., Wunder, T., Pesaresi, P., Pribil, M., Armbruster, U. and Leister, D. (2013) PGRL1 is the elusive ferredoxin-plastoquinone reductase in photosynthetic cyclic electron flow. *Mol Cell*, **49**, 511-523.

Hou, C.X., Rintamaki, E. and Aro, E.M. (2003) Ascorbate-mediated LHCII protein phosphorylation--LHCII kinase regulation in light and in darkness. *Biochemistry*, **42**, 5828-5836.

Ifuku, K., Endo, T., Shikanai, T. and Aro, E.M. (2011a) Structure of the chloroplast NADH dehydrogenase-like complex: nomenclature for nuclear-encoded subunits. *Plant Cell Physiol*, **52**, 1560-1568.

Ifuku, K., Ido, K. and Sato, F. (2011b) Molecular functions of PsbP and PsbQ proteins in the photosystem II supercomplex. *J Photochem Photobiol B*, **104**, 158-164.

Ifuku, K., Ishihara, S. and Sato, F. (2010) Molecular functions of oxygen-evolving complex family proteins in photosynthetic electron flow. *J Integr Plant Biol*, **52**, 723-734.

Ihnatowicz, A., Pesaresi, P., Varotto, C., Richly, E., Schneider, A., Jahns, P., Salamini, F. and Leister, D. (2004) Mutants for photosystem I subunit D of Arabidopsis thaliana: effects on photosynthesis, photosystem I stability and expression of nuclear genes for chloroplast functions. *Plant J*, **37**, 839-852.

Jarvi, S., Suorsa, M., Paakkarinen, V. and Aro, E.M. (2011) Optimized native gel systems for separation of thylakoid protein complexes: novel super- and mega-complexes. *Biochem J*, **439**, 207-214.

Jensen, P.E., Gilpin, M., Knoetzel, J. and Scheller, H.V. (2000) The PSI-K subunit of photosystem I is involved in the interaction between light-harvesting complex I and the photosystem I reaction center core. *J Biol Chem*, **275**, 24701-24708.

Johnson, G.N. (2011) Physiology of PSI cyclic electron transport in higher plants. *Biochim Biophys Acta*, **1807**, 384-389.

Joliot, P. and Johnson, G.N. (2011) Regulation of cyclic and linear electron flow in higher plants. *Proc Natl Acad Sci U S A*, **108**, 13317-13322.

Joliot, P. and Joliot, A. (2002) Cyclic electron transfer in plant leaf. *Proc Natl Acad Sci U S A*, **99**, 10209-10214.

Kono, M., Noguchi, K. and Terashima, I. (2014) Roles of the cyclic electron flow around PSI (CEF-PSI) and O(2)-dependent alternative pathways in regulation of the photosynthetic electron flow in short-term fluctuating light in Arabidopsis thaliana. *Plant Cell Physiol*, **55**, 990-1004.

Kotera, E., Tasaka, M. and Shikanai, T. (2005) A pentatricopeptide repeat protein is essential for RNA editing in chloroplasts. *Nature*, **433**, 326-330.

Leister, D. and Shikanai, T. (2013) Complexities and protein complexes in the antimycin A-sensitive pathway of cyclic electron flow in plants. *Front Plant Sci*, **4**, 161.

Leister, D., Varotto, C., Pesaresi, P., Niwergall, A. and Salamini, F. (1999) Large-scale evaluation of plant growth in Arabidopsis thaliana by non-invasive image analysis. *Plant Physiol Bioch*, **37**, 671-678.

Li, X.P., Bjorkman, O., Shih, C., Grossman, A.R., Rosenquist, M., Jansson, S. and Niyogi, K.K. (2000) A pigment-binding protein essential for regulation of photosynthetic light harvesting. *Nature*, **403**, 391-395.

Lundin, B., Hansson, M., Schoefs, B., Vener, A.V. and Spetea, C. (2007) The Arabidopsis PsbO2 protein regulates dephosphorylation and turnover of the photosystem II reaction centre D1 protein. *Plant J*, **49**, 528-539.

Lundin, B., Nurmi, M., Rojas-Stuetz, M., Aro, E.M., Adamska, I. and Spetea, C. (2008) Towards understanding the functional difference between the two PsbO isoforms in Arabidopsis thaliana--insights from phenotypic analyses of psbo knockout mutants. *Photosynth Res*, **98**, 405-414.

Majeran, W. and van Wijk, K.J. (2009) Cell-type-specific differentiation of chloroplasts in C4 plants. *Trends Plant Sci*, **14**, 100-109.

Martinez-Garcia, J.F., Monte, E. and Quail, P.H. (1999) A simple, rapid and quantitative method for preparing Arabidopsis protein extracts for immunoblot analysis. *Plant Journal*, **20**, 251-257.

McDonald, A.E., Ivanov, A.G., Bode, R., Maxwell, D.P., Rodermel, S.R. and Huner, N.P. (2011) Flexibility in photosynthetic electron transport: the physiological role of plastoquinol terminal oxidase (PTOX). *Biochim Biophys Acta*, **1807**, 954-967.

Munekage, Y., Hashimoto, M., Miyake, C., Tomizawa, K., Endo, T., Tasaka, M. and Shikanai, T. (2004) Cyclic electron flow around photosystem I is essential for photosynthesis. *Nature*, **429**, 579-582.

Munekage, Y., Hojo, M., Meurer, J., Endo, T., Tasaka, M. and Shikanai, T. (2002) PGR5 is involved in cyclic electron flow around photosystem I and is essential for photoprotection in Arabidopsis. *Cell*, **110**, 361-371.

Murakami, R., Ifuku, K., Takabayashi, A., Shikanai, T., Endo, T. and Sato, F. (2002) Characterization of an Arabidopsis thaliana mutant with impaired psbO, one of two genes encoding extrinsic 33-kDa proteins in photosystem II. *FEBS Lett*, **523**, 138-142.

Murakami, R., Ifuku, K., Takabayashi, A., Shikanai, T., Endo, T. and Sato, F. (2005) Functional dissection of two Arabidopsis PsbO proteins: PsbO1 and PsbO2. *Febs J*, **272**, 2165-2175.

Ogawa, T. and Mi, H. (2007) Cyanobacterial NADPH dehydrogenase complexes. *Photosynth Res*, **93**, 69-77.

Peng, L., Yamamoto, H. and Shikanai, T. (2011) Structure and biogenesis of the chloroplast NAD(P)H dehydrogenase complex. *Biochim Biophys Acta*, **1807**, 945-953.

Pesaresi, P., Hertle, A., Pribil, M., Kleine, T., Wagner, R., Strissel, H., Ihnatowicz, A., Bonardi, V., Scharfenberg, M., Schneider, A., Pfannschmidt, T. and Leister, D. (2009) Arabidopsis STN7 kinase provides a link between short- and long-term photosynthetic acclimation. *Plant Cell*, **21**, 2402-2423.

Pesaresi, P., Pribil, M., Wunder, T. and Leister, D. (2011) Dynamics of reversible protein phosphorylation in thylakoids of flowering plants: the roles of STN7, STN8 and TAP38. *Biochim Biophys Acta*, **1807**, 887-896.

Pietrzykowska, M., Suorsa, M., Semchonok, D.A., Tikkanen, M., Boekema, E.J., Aro, E.M. and Jansson, S. (2014) The Light-Harvesting Chlorophyll a/b Binding Proteins Lhcb1 and Lhcb2 Play Complementary Roles during State Transitions in Arabidopsis. *Plant Cell*, **26**, 3646-3660.

Popelkova, H., Commet, A., Kuntzleman, T. and Yocum, C.F. (2008) Inorganic cofactor stabilization and retention: the unique functions of the two PsbO subunits of eukaryotic photosystem II. *Biochemistry*, **47**, 12593-12600.

Pribil, M., Pesaresi, P., Hertle, A., Barbato, R. and Leister, D. (2010) Role of plastid protein phosphatase TAP38 in LHCII dephosphorylation and thylakoid electron flow. *PLoS Biol*, **8**, e1000288.

Rochaix, J.D., Lemeille, S., Shapiguzov, A., Samol, I., Fucile, G., Willig, A. and Goldschmidt-Clermont, M. (2012) Protein kinases and phosphatases involved in the acclimation of the photosynthetic apparatus to a changing light environment. *Philos Trans R Soc Lond B Biol Sci*, **367**, 3466-3474.

Sacksteder, C.A., Kanazawa, A., Jacoby, M.E. and Kramer, D.M. (2000) The proton to electron stoichiometry of steady-state photosynthesis in living plants: A proton-pumping Q cycle is continuously engaged. *Proceedings of the National Academy of Sciences*, **97**, 14283-14288.

Samol, I., Shapiguzov, A., Ingelsson, B., Fucile, G., Crevecoeur, M., Vener, A.V., Rochaix, J.D. and Goldschmidt-Clermont, M. (2012) Identification of a photosystem II phosphatase involved in light acclimation in Arabidopsis. *Plant Cell*, **24**, 2596-2609.

Schagger, H. and Vonjagow, G. (1987) Tricine Sodium Dodecyl-Sulfate Polyacrylamide-Gel Electrophoresis for the Separation of Proteins in the Range from 1-Kda to 100-Kda. *Anal Biochem*, **166**, 368-379.

Shapiguzov, A., Ingelsson, B., Samol, I., Andres, C., Kessler, F., Rochaix, J.D., Vener, A.V. and Goldschmidt-Clermont, M. (2010) The PPH1 phosphatase is specifically involved in LHCII dephosphorylation and state transitions in Arabidopsis. *Proc Natl Acad Sci U S A*, **107**, 4782-4787.

Shikanai, T. (2014) Central role of cyclic electron transport around photosystem I in the regulation of photosynthesis. *Curr Opin Biotechnol*, **26**, 25-30.

Shimizu, H., Peng, L., Myouga, F., Motohashi, R., Shinozaki, K. and Shikanai, T. (2008) CRR23/NdhL is a subunit of the chloroplast NAD(P)H dehydrogenase complex in Arabidopsis. *Plant Cell Physiol*, **49**, 835-842.

Shutova, T., Nikitina, J., Deikus, G., Andersson, B., Klimov, V. and Samuelsson, G. (2005) Structural dynamics of the manganese-stabilizing protein-effect of pH, calcium, and manganese. *Biochemistry*, **44**, 15182-15192.

Suorsa, M., Jarvi, S., Grieco, M., Nurmi, M., Pietrzykowska, M., Rantala, M., Kangasjarvi, S., Paakkarinen, V., Tikkanen, M., Jansson, S. and Aro, E.M. (2012) PROTON GRADIENT REGULATION5 is essential for proper acclimation of Arabidopsis photosystem I to naturally and artificially fluctuating light conditions. *Plant Cell*, **24**, 2934-2948.

Suorsa, M., Sirpio, S., Allahverdiyeva, Y., Paakkarinen, V., Mamedov, F., Styring, S. and Aro, E.M. (2006) PsbR, a missing link in the assembly of the oxygen-evolving complex of plant photosystem II. *J Biol Chem*, **281**, 145-150.

Tikkanen, M. and Aro, E.M. (2012) Thylakoid protein phosphorylation in dynamic regulation of photosystem II in higher plants. *Biochim Biophys Acta*, **1817**, 232-238.

Tikkanen, M., Piippo, M., Suorsa, M., Sirpio, S., Mulo, P., Vainonen, J., Vener, A.V., Allahverdiyeva, Y. and Aro, E.M. (2006) State transitions revisited-a buffering system for dynamic low light acclimation of Arabidopsis. *Plant Mol Biol*, **62**, 779-793.

Wang, C., Yamamoto, H. and Shikanai, T. (2014) Role of cyclic electron transport around photosystem I in regulating proton motive force. *Biochim Biophys Acta*.

Willig, A., Shapiguzov, A., Goldschmidt-Clermont, M. and Rochaix, J.D. (2011) The phosphorylation status of the chloroplast protein kinase STN7 of Arabidopsis affects its turnover. *Plant Physiol*, **157**, 2102-2107.

Xu, Q. and Bricker, T.M. (1992) Structural organization of proteins on the oxidizing side of photosystem II. Two molecules of the 33-kDa manganese-stabilizing proteins per reaction center. *J Biol Chem*, **267**, 25816-25821.

Yamamoto, H., Peng, L., Fukao, Y. and Shikanai, T. (2011) An Src homology 3 domain-like fold protein forms a ferredoxin binding site for the chloroplast NADH dehydrogenase-like complex in Arabidopsis. *Plant Cell*, **23**, 1480-1493.

Yi, X., McChargue, M., Laborde, S., Frankel, L.K. and Bricker, T.M. (2005) The manganese-stabilizing protein is required for photosystem II assembly/stability and photoautotrophy in higher plants. *J Biol Chem*, **280**, 16170-16174.

Yin, L., Fristedt, R., Herdean, A., Solymosi, K., Bertrand, M., Andersson, M.X., Mamedov, F., Vener, A.V., Schoefs, B. and Spetea, C. (2012) Photosystem II function and dynamics in three widely used Arabidopsis thaliana accessions. *PLoS One*, **7**, e46206.

Figures and Legends

A

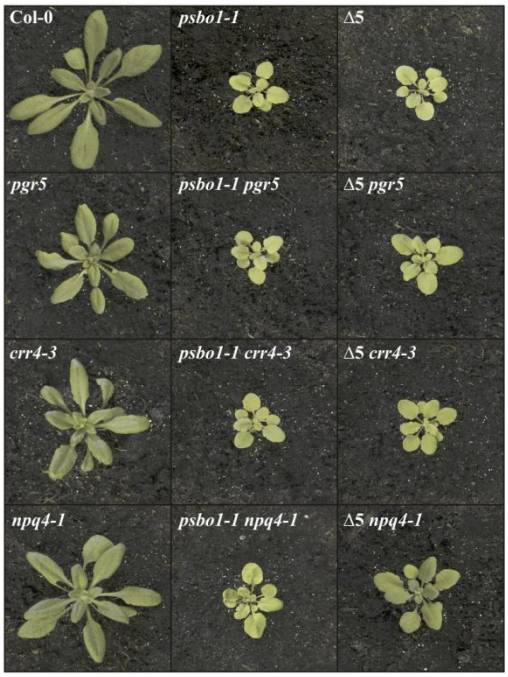

B

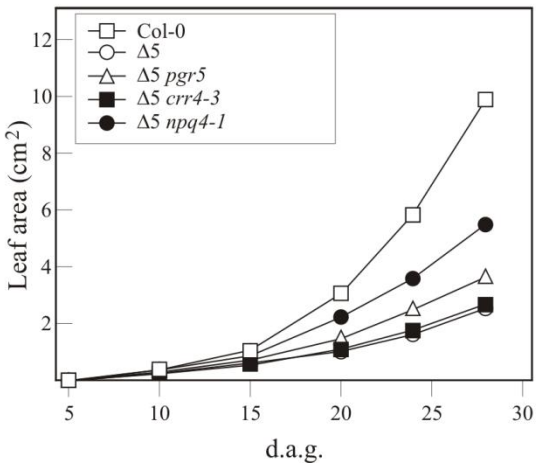

Figure 1. Phenotypes of WT (Col-0), single-, and multiple-mutant plants with reduced OEC function combined with defects in CET and NPQ. (A) All genotypes were grown for four weeks under optimal conditions in growth chambers. (B) Growth kinetics of Col-0, the quintuple OEC mutant *psbo1-1 psbp2-1 psbq1-1 psbq2-1 psbr-1* (D5) and the sextuple mutants D5 *pgr5*, D5 *crr4-3*,

D5 *npq4-1* were measured from 5 to 28 days after germination (d.a.g.). Each point is based on the determination of mean leaf area in at least 10 individuals (n ³ 10). Standard deviations were below 10%. Growth kinetics of the *psbo1-1* single mutant, and double mutants affected in either CET (*psbo1-1 pgr5*, *psbo1-1 crr4-3*) or NPQ (*psbo1-1 npq4-1*) were also measured, but did not differ from WT.

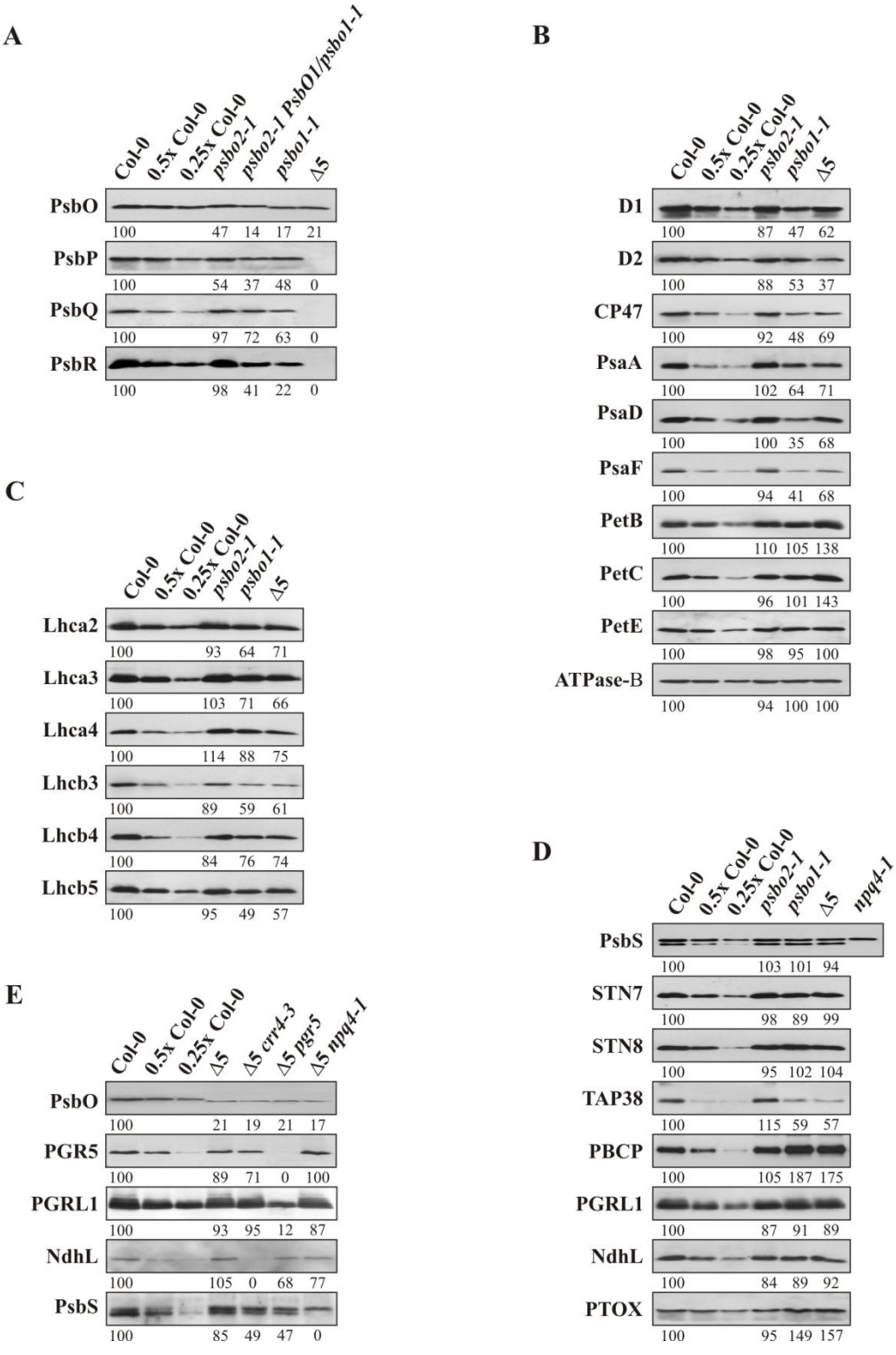

Figure 2. Immunoblot analyses of thylakoid protein complexes in Col-0 and mutant leaves with altered OEC protein composition. (A) PVDF filters bearing fractionated total proteins, isolated at the 8-leaf rosette stage from WT and mutant plants, were probed with antibodies raised against individual subunits of OEC (PsbO, PsbP, PsbQ and PsbR). (B) Samples from the same set of genotypes probed with antibodies specific for PSII (D1, D2, CP47), PSI (PsaA, PsaD, PsaF), Cyt

b_6/f (PetB, PetC), plastocyanin (PetE) and the beta subunit of ATPase (ATPase-B). (C) Amounts of PSI-specific (Lhca2, Lhca3, Lhca4) and PSII-specific antenna proteins (Lhcb3, Lhcb4, Lhcb5) in the same set of genotypes. (D) Levels of factors involved in the following short-term regulatory responses of photosynthesis: NPQ (PsbS), thylakoid protein phosphorylation (STN7, STN8, TAP38/PPH1, PBCP), alternative electron transport (PGRL1, NdhL, PTOX). Note that PsbO2 abundance is not influenced by the introduction of *pgr5*, *crr4-3* and *npq4-1* mutations into the D5 background. Protein abundance as a percentage of the WT level is given below each immunoblot. It has to be considered that loading of identical protein amounts might lead to overestimation of thylakoid protein abundances in plants with marked alteration of photosynthetic performance, such as *psbo1-1* and D5, when compared to WT.

A

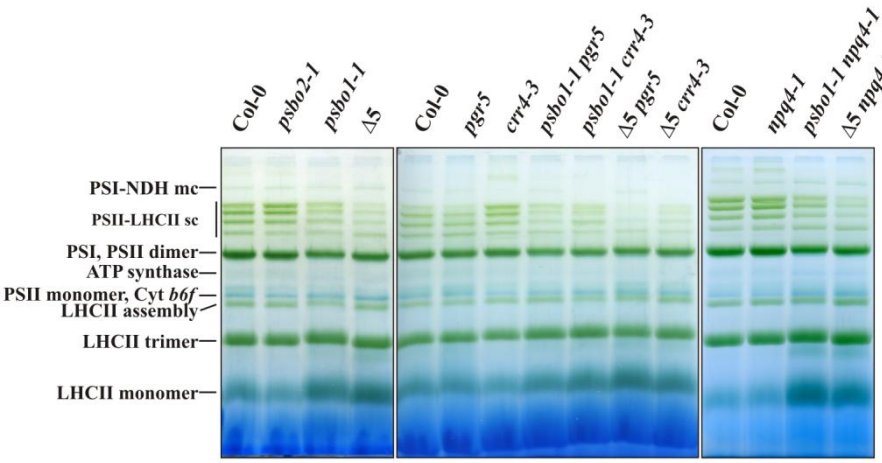
Col-0
psbo2-1
psbo1-1
Δ5
Col-0
pgr5
crr4-3
psbo1-1 pgr5
psbo1-1 crr4-3
Δ5 pgr5
Δ5 crr4-3
Col-0
npq4-1
psbo1-1 npq4-1
Δ5 npq4-1
PSI-NDH mc
PSII-LHCII sc
PSI, PSII dimer
ATP synthase
PSII monomer, Cyt b6f
LHCII assembly
LHCII trimer
LHCII monomer

B

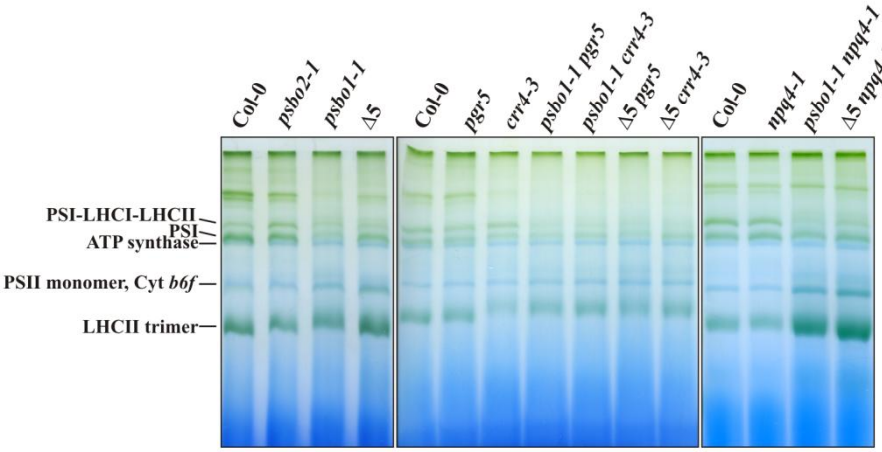
Col-0
psbo2-1
psbo1-1
Δ5
Col-0
pgr5
crr4-3
psbo1-1 pgr5
psbo1-1 crr4-3
Δ5 pgr5
Δ5 crr4-3
Col-0
npq4-1
psbo1-1 npq4-1
Δ5 npq4-1
PSI-LHCI-LHCII
PSI
ATP synthase
PSII monomer, Cyt b6f
LHCII trimer

C

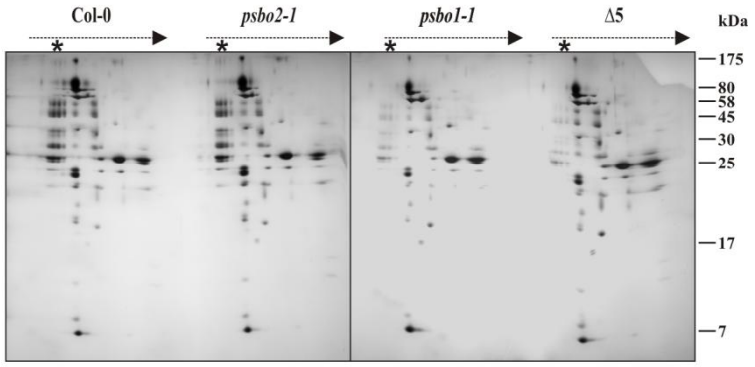
Col-0
psbo2-1
psbo1-1
Δ5
kDa
175
80
58
45
30
25
17
7

D

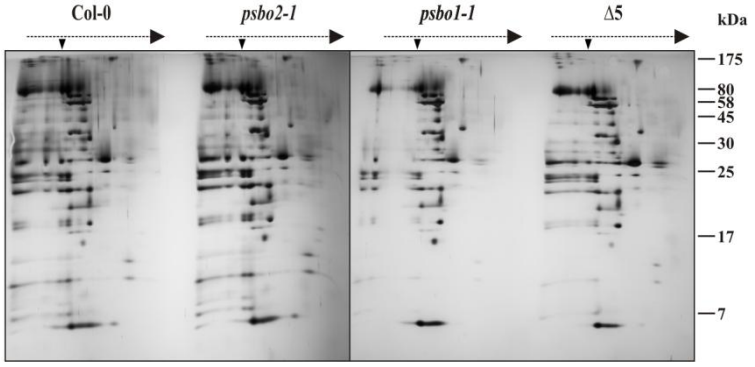
Col-0
psbo2-1
psbo1-1
Δ5
kDa
175
80
58
45
30
25
17
7

Figure 3. Blue Native and 2D SDS-PAGE analyses of thylakoid membrane protein complexes in Col-0, single and quintuple OEC mutants (*psbo1-1*, *psbo2-1*, D5), and in quintuple mutants devoid of NPQ (D5 *npq4-1*) or CET (D5 *pgr5*, D5 *crr4-3*). (A) Thylakoid membranes were isolated from mature Col-0 and mutant plants at the 8-leaf rosette stage, and solubilised with 1% (w/v) β-dodecyl maltoside prior to fractionation by large-pore Blue Native PAGE (lpBN-PAGE) (B) Thylakoid membranes isolated from the same set of genotypes were also solubilised with 1% (w/v) digitonin and fractionated by lpBN-PAGE. (C) The BN gel lanes from Col-0, *psbo1-1*, *psbo2-1*, D5 shown in (A) were subjected to denaturing PAGE, and the 2D gels were stained with silver. (D) The BN gels lanes from Col-0, *psbo1-1*, *psbo2-1*, D5 shown in (B) were fractionated and stained as in (C). NDH, NAD(P)H dehydrogenase; PS, photosystems; LHC, light-harvesting complex; Cyt b_6f, cytochrome b_6f; sc, supercomplex; mc, megacomplex.

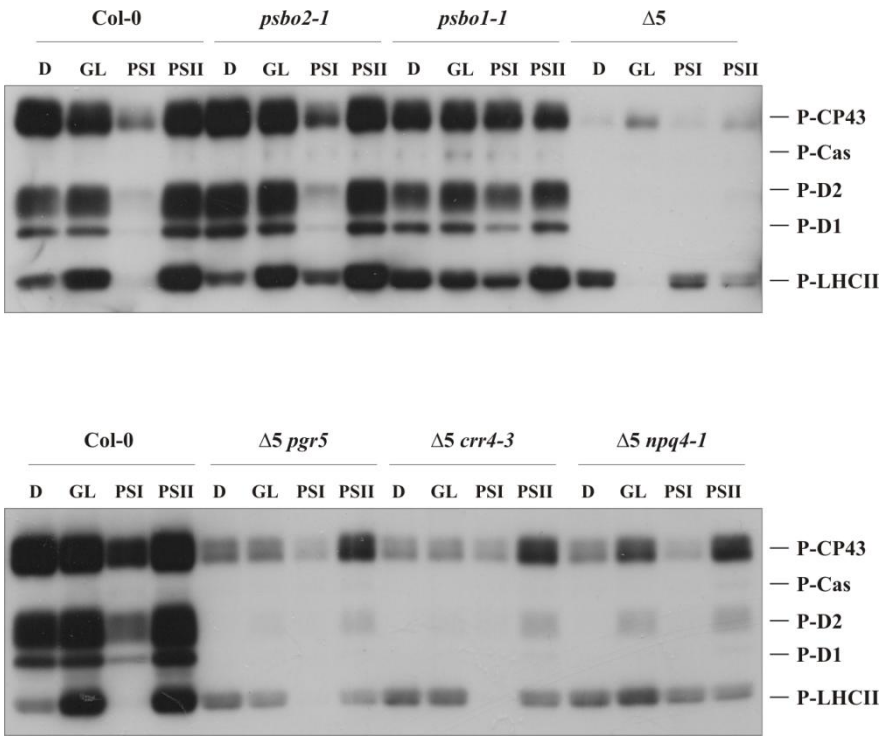

Figure 4. Thylakoid protein phosphorylation in Col-0 and mutant plants. Thylakoid proteins extracted from leaves (8-leaf rosette stage) of Col-0 and mutant mature plants kept overnight in the dark (D), and subsequently exposed to growth light (GL), PSI-enriched light (PSI) or PSII-enriched light, were fractionated by SDS-PAGE, transferred to PVDF membranes and probed with a polyclonal anti-phosphothreonine antibody. Levels of phosphorylation of LHCII (P-LHCII), Cas (P-Cas) and PSII core proteins (P-D1, P-D2 and P-CP43) detected on one representative immunoblot (*n*=3) for each genotype are shown.

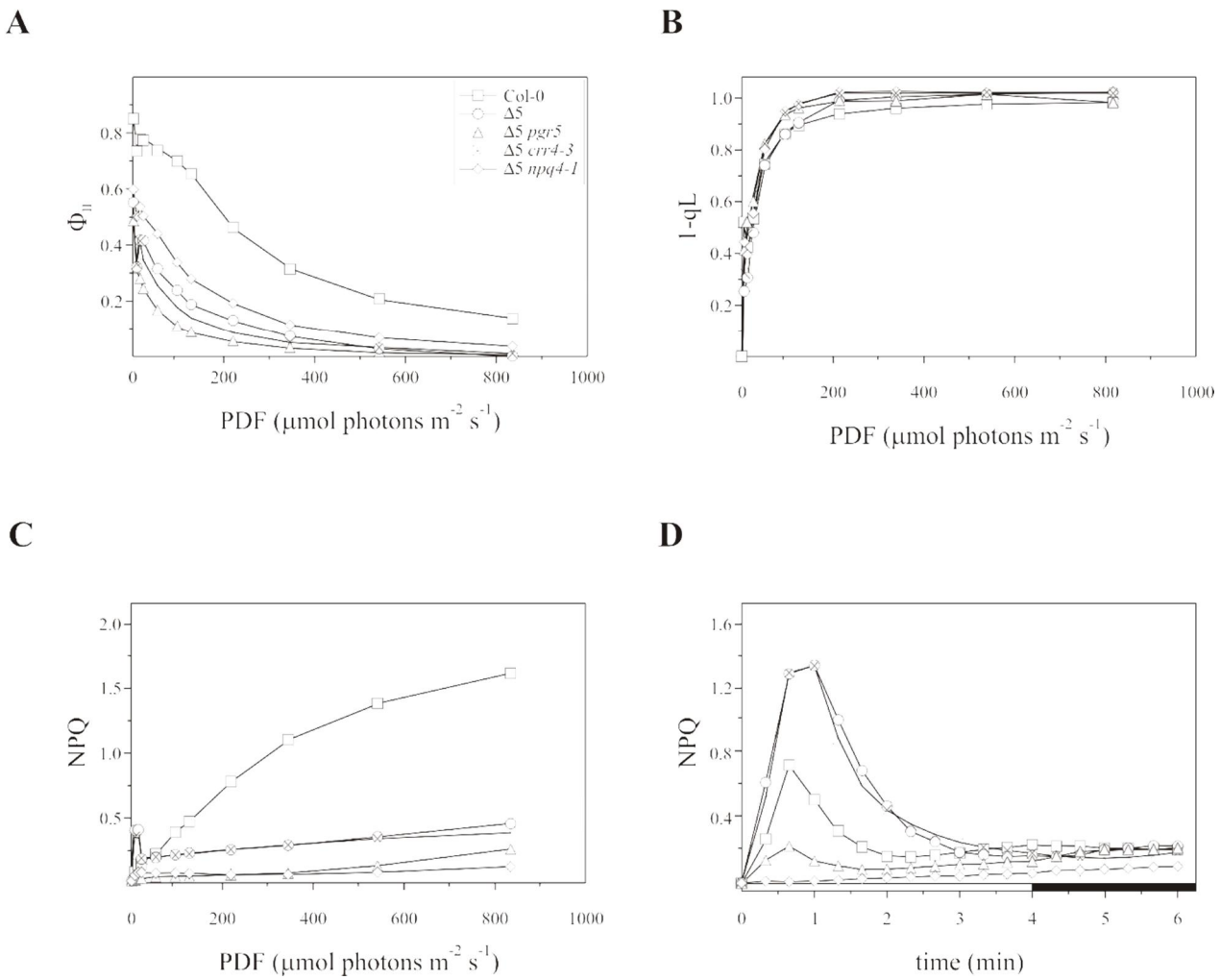

Figure 5. Photosynthetic performance of WT (Col-0) and mutant plants. (A) The photosynthetic parameters F_V/F_M (dark adapted), Φ_{II} (light adapted), (B) 1-qL and (C) steady-state NPQ were measured at the 8-leaf rosette stage in WT and mutant plants grown under low light conditions (80 µmol photons m^{-2} sec^{-1}), dark-adapted for 30 min and illuminated for 2 min with various light intensities. Fluorescence was recorded after dark adaptation and at the end of each illumination period (PDF, photosynthetically active flux density). (D) Time courses of induction and relaxation of NPQ monitored during the dark-to-light (53 µmol photons m^{-2} sec^{-1}, white bar) transition. The 4-min light period (white bar) was followed by a 2-min dark period (black bar). Note that NPQ induction during activation of photosynthesis is thought to be caused by the transient acidification of the thylakoid lumen associated with high CET activity and low CO_2 assimilation, which reduces DpH consumption for ATP synthesis.

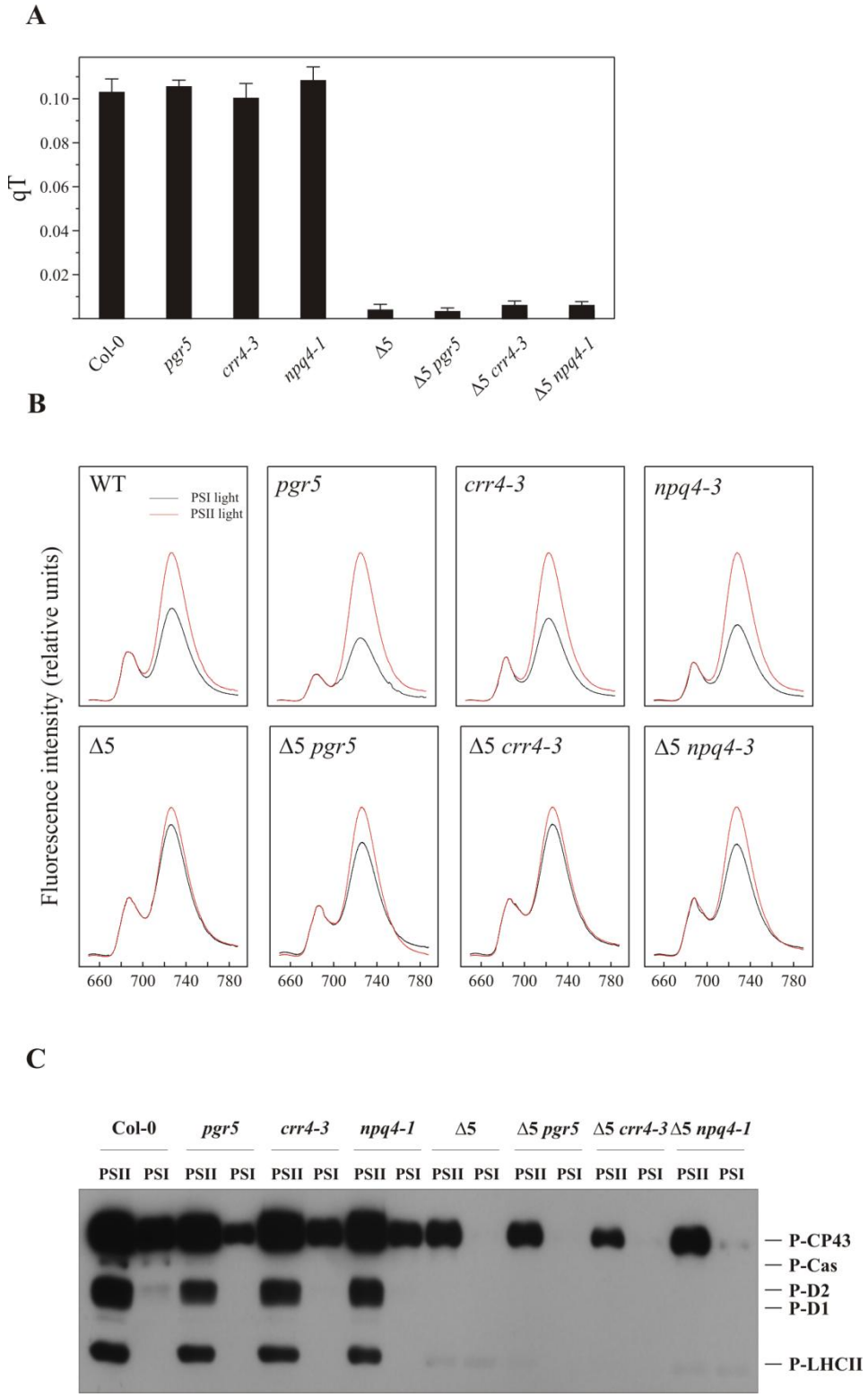

Figure 6. State Transitions in WT (Col-0) and mutant plants. (A) Quenching of chlorophyll fluorescence due to state transitions (qT; see also Methods). Mean values obtained from five independent measurements for each genotype are reported. Bars indicate standard deviations. (B) Low-temperature (77 K) chlorophyll a fluorescence emission spectra of thylakoids after 1 hour exposure of plants to light inducing either state 1 (black lines, far-red light: 30 µmol photons m^{-2}

sec^{-1}) or state 2 (red lines, red light; 50 µmol photons m^{-2} sec^{-1}) (see also Methods). The excitation wavelength was 475 nm, and spectra were normalized with reference to peak height at 685 nm. Traces are the average of 5 replicates. (C) Thylakoids as in (B) were fractionated by SDS-PAGE, transferred to PVDF membranes and probed with a polyclonal anti-phosphothreonine antibody. Levels of phosphorylation of LHCII (P-LHCII), Cas (P-Cas) and PSII core proteins (P-D1, P-D2 and P-CP43) detected on one representative immunoblot (*n*=3) for each genotype are shown.

A

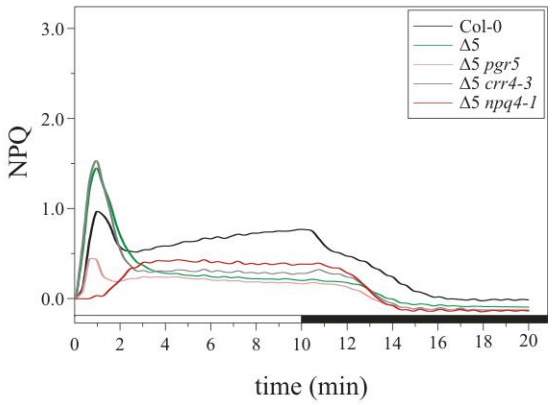

B

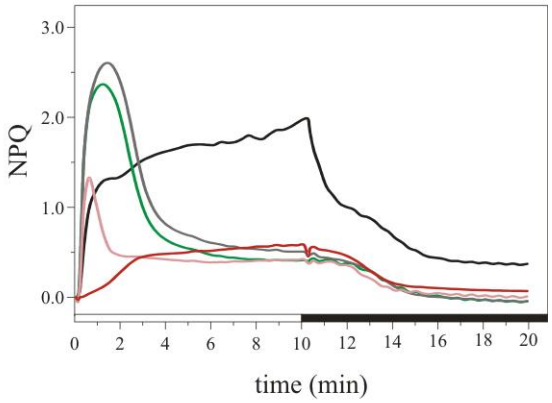

C

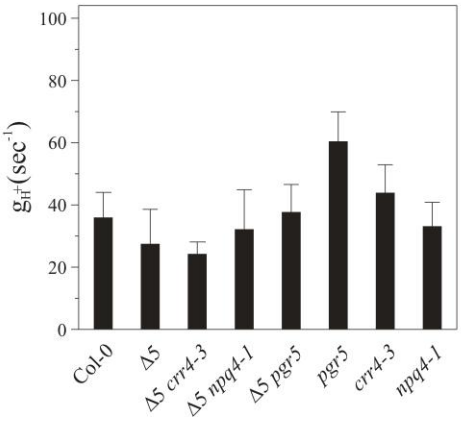

Figure 7. NPQ induction and proton conductivity of thylakoid ATPase (g_H^+) in WT (Col-0) and mutant leaves. Fluorescence imaging at room temperature was performed upon transfer from the dark to light levels of either 90 (A) or 600 µmol photons m^{-2} sec^{-1} (B) for 10 min (white bar), followed by a dark period of 10 min (black bar). Intact plants were imaged and mean values for 15 leaves per genotype were calculated. (C) Estimates of g_H^+ were obtained by taking the inverse of the time constant for Electrochromic Shift (ECS) relaxation kinetics in the dark after leaf exposure for

120 sec to red light (see also Methods). Mean values for 12 leaves for genotype were calculated. Bars represent standard deviation.

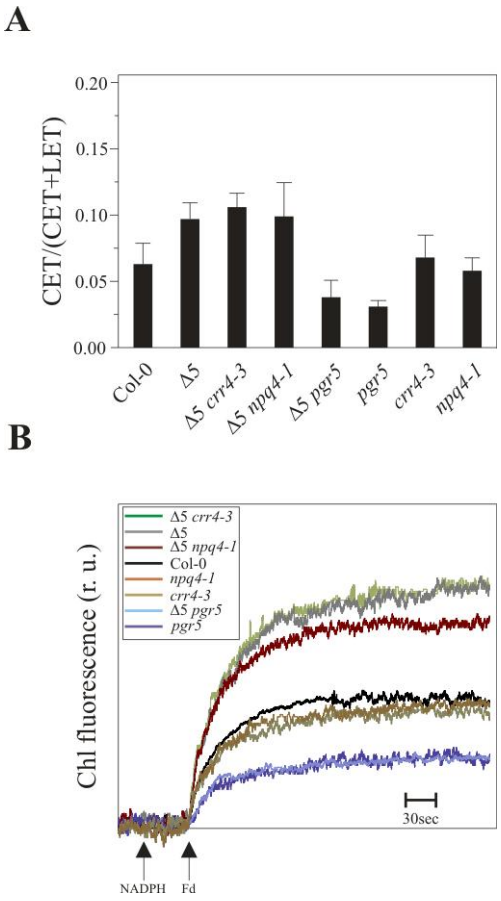

Figure 8. *In vivo* measurements of CET rates. (A) Electrochromic Shift (ECS) spectral changes were employed to evaluate LET and CET rates in WT (Col-0) and mutant plants. Linear and cyclic electron flow rates were calculated from the relaxation kinetics of the ECS signals in the dark after exposure for 120 sec to red (600 µmol photons m^{-2} sec^{-1}; LET rate) and saturating far-red light (CET rate). (B) Quantification of CET rates by measuring the increases in chlorophyll fluorescence in ruptured chloroplasts under low measuring light (1 $\mu E/m^2s^{-1}$) , after the addition of NADPH and Fd, according to the method described in Munekage et al. (2002).

A

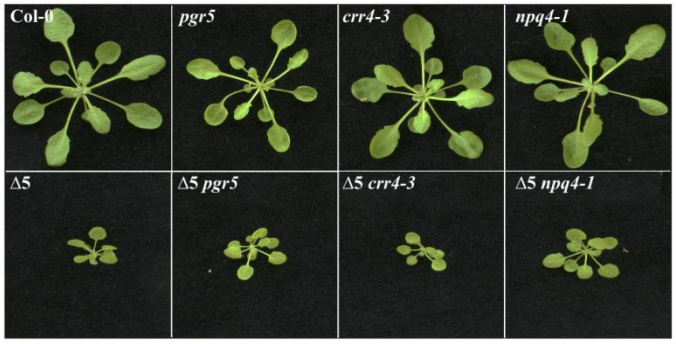

B

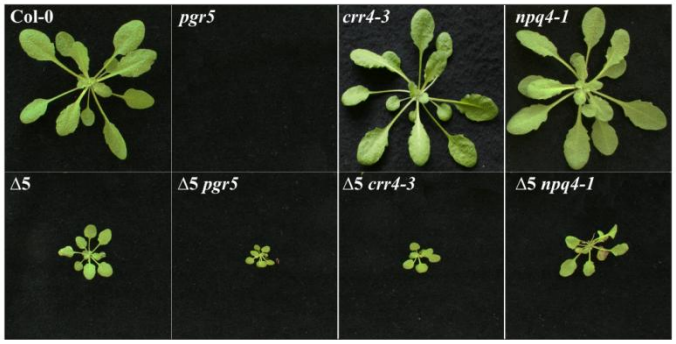

Figure 9. Phenotypes of WT (Col-0) and mutant plants grown under constant and fluctuating light conditions. WT and mutant plants were grown for 4 weeks (A) under constant light (200 µmol photons m^{-2} sec^{-1}) or (B) under fluctuating light [cycles of 5 min of low light (50 µmol photons m^{-2} sec^{-1}) followed by 1 min of high light (500 µmol photons m^{-2} sec^{-1}) repeated over the entire photoperiod]. Note that *pgr5* plants do not progress beyond the seedling stage under fluctuating light. All plant material was grown in a growth chamber under the photoperiod of 8h light/16h dark.

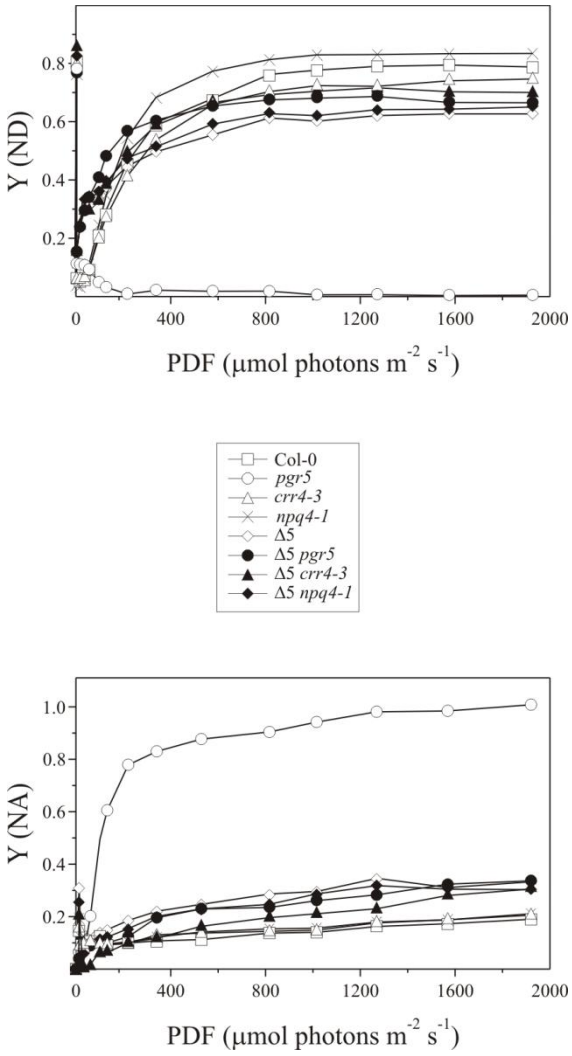

Figure 10. *In vivo* measurements of PSI donor side [Y(ND)] and acceptor side [Y(NA)] limitations. Variations in Y(ND) and Y(NA) were monitored in WT (Col-0) and mutant plants by measuring the redox state of P700 at room temperature under different light intensities with the Dual-PAM-100 (Walz). Note that the constitutive reduction of P700 in *pgr5* leaves under all light intensities tested, is almost fully rescued in D5 *pgr5* mutant leaves.

Tables

Table 1. Levels of leaf pigments in light-adapted mutant and Col-0 plants at the 8-leaf rosette stage. Leaf pigments were assayed by HPLC and are reported in pmol/mg leaf fresh weight. Mean values ± SD are shown. Nx, neoxanthin; Lut, lutein; Chl b, chlorophyll b; Chl a, chlorophyll a; β-Car, β-carotene; VAZ, violaxanthin + antheraxanthin + zeaxanthin. Levels of leaf pigments in light-adapted Col-0 and OEC mutant plants.

	Nx	Lut	β-Car	VAZ	Chl a+b
Col-0	77 ± 5	226 ± 20	198 ± 13	59 ± 8	2301 ± 146
psbo2-1	72 ± 5	213 ± 19	181 ± 33	60 ± 5	2268 ± 89
psbo1-1	44 ± 4	136 ± 10	61 ± 7	33 ± 5	1678 ± 65
D5	46 ± 4	134 ± 10	64 ± 6	32 ± 4	1681 ± 73
D5 *pgr5*	46 ± 4	149 ± 8	63 ± 5	37 ± 5	1739 ± 83
D5 *crr4-3*	51 ± 6	165 ± 10	61 ± 4	29 ± 4	1815 ± 110
D5 *npq4-1*	66 ± 5	200 ± 12	81 ± 4	49 ± 3	2063 ± 98

Table 2. Summary of the main characteristics (relative to WT) of the mutants used in this study. / = absent; - - = reduction between 100 and 50%; - = reduction between 50 and 0%; 0 = identical to WT; + = upregulation between 0 and 50%; ++ = upregulation by more than 50%. FL = fluctuating light; Nd = not determined. Note that the characteristics of *psbo2-1 PsbO1/psbo1-1* plants are intermediate between *psbo2-1* and *psbo1-1*, whereas *psbo1-1 psbo2-1* plants are inviable even under optimal growth conditions. To reduce the complexity of the Table, the characteristics of the double mutants *psbo1-1 pgr5*, *psbo1-1 crr4-3* and *psbo1-1 npq4-1* were not included. sc = supercomplexes.

		psbo2-1	*psbo1-1*	D5	D5 *crr4-3*	D5 *pgr5*	D5 *npq4-1*	Figures/Tables
Phenotype	Growth rate	0	--	--	--	--[1]	-	1 and S1
	Chl a + b	0	-	-	-	-	-	Table 1
OEC proteins	PsbO1	--	/	/	/	/	/	2
	PsbO2	/	--	--	--	--	--	2
	PsbP	-	--	/	/[2]	/	/	2
	PsbQ	-	-	/	/	/	/	2
	PsbR	0	--	/	/	/	/	2
Thylakoid protein complexes	PSI	0	--[3]	-	nd	nd	nd	2 and 3
	PSII	-	--	-[4]	nd	nd	nd	2 and 3
	Cyt b_6f	0	0	+	nd	nd	nd	2 and 3
	ATPase	0	0	0	nd	nd	nd	2 and 3
Antenna proteins	Lhca	0	-	-	nd	nd	nd	2 and 3
	Lhcb	-	-	-	nd	nd	nd	2 and 3
Regulatory proteins	STN kinases	0	0	0	nd	nd	nd	2
	TAP38/PPH1	+	-	-	nd	nd	nd	2
	PBCP	0	++	++	nd	nd	nd	2
Photosystem	PSII-LHCII sc	0	--	--	--	--	--	3

supercomplexes	PSI-LHCI-LHCII	0	--	--	--	--	--	3
Phosphorylation: GL-light	P-PSII core	0	-	/[5]	/	/	-	4
	P-LHCII	0	-	/	--	--	--	4
Phosphorylation: PSI-light	P-PSII core	+	++	0	0	0	0	4
	P-LHCII	++	++	++	0	0	+	4
Functional characteristics	PSII Yield[6]	0	--	--	--	--	-	5 and S4
	Transient NPQ[7]	0	+	++	++	--	/	5 and S4
	Steady state NPQ[6]	0	--	--	--	/	/	5 and S4
	CET	nd	nd	++	++	-	+	7
	State Transitions	0	-	--	--	--	--	5 and S4

[1]Note that the *pgr5* single mutant dies at the seedling stage under fluctuating light, whereas Δ5 *pgr5* plants are viable (Figure 8)

[2]The levels of OEC subunits in Δ5 *pgr5*, Δ5 *crr4-3* and Δ5 *npq4-1* were identical to those in Δ5 leaves (Figure 2 and data not shown)

[3]Note that the PSI core subunit PsaA was less severely down-regulated relative to the peripheral subunits PsaD and PsaF (Figure 2)

[4]Note that the PSII core subunit D2 was more severely reduced than D1 and CP47

[5]Only very limited phosphorylation of CP43 was observed in Δ5, Δ5 *pgr5* and Δ5 *crr4-3* leaves

[6]Values refer to 200 µmol photons m^{-2} sec^{-1} of actinic light

[7]Values refer to 1 min of light exposure (see also Figure 6)

Supplemental materials

A

B

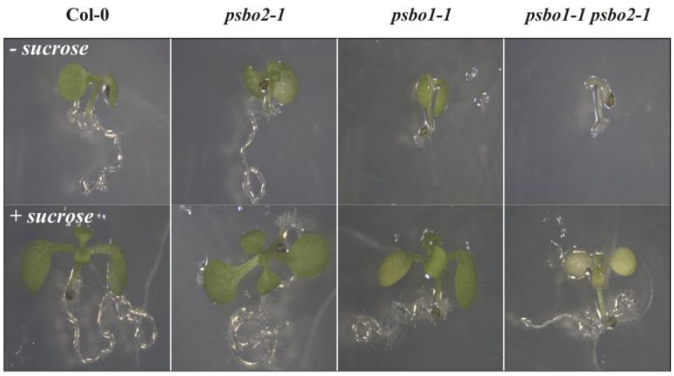

C

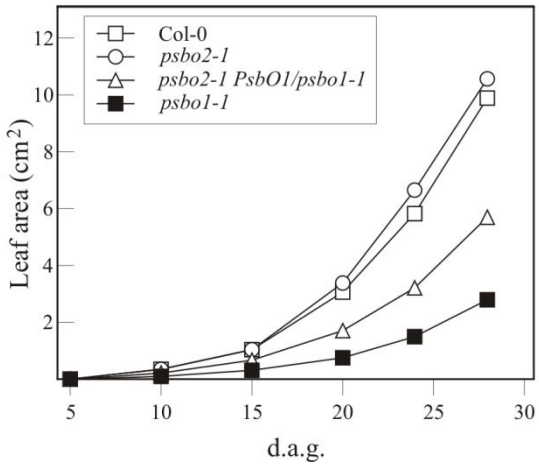

Figure S1. Phenotypes of Col-0 (WT) and *psbo1-1*, *psbo2-1* and *psbo2-1 PsbO1/psbo1-1* mutants characterized by reduced contents of PsbO protein. (A) Col-O and mutant plants were grown on soil for 4 weeks in a growth chamber. (B) Col-0, *psbo1-1*, *psbo2-1* and the double mutant *psbo1-1 psbo2-1* were grown for 10 days on MS medium supplemented or not with 1% sucrose. (C) Growth curves measured from 5 to 28 d.a.g. Leaf area values are the means of measurements made on at least 10 independent leaves (n ³ 10). Standard deviations were below 10%.

Figure S2. Comparison of Arabidopsis PsbO1 (At5g66570) and PsbO2 (At3g50820) sequences. Black boxes indicate strictly conserved amino acids and grey boxes closely related ones. The arrowhead indicates the N-terminal residues of the mature proteins. Asterisks indicate residues that account for the functional differences between the two PsbO isoforms (Murakami, *et al.* 2005).

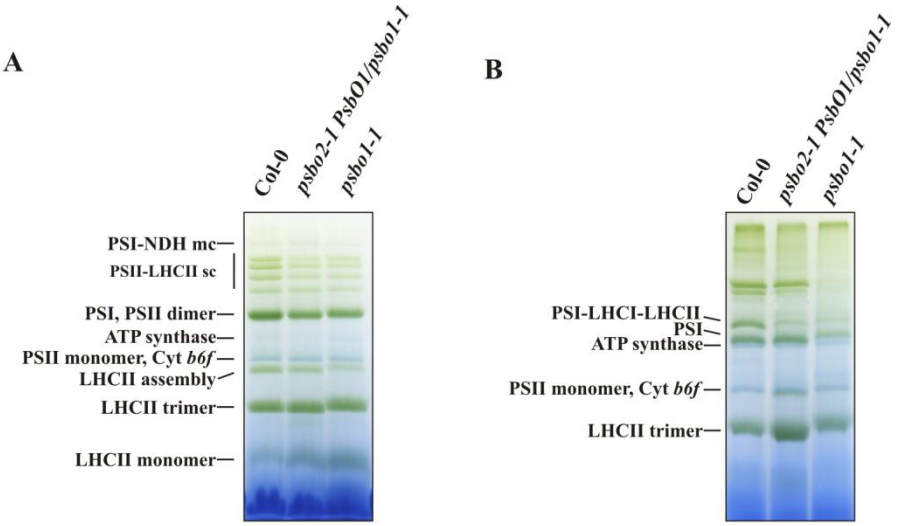
A
Col-0
psbo2-1 PsbO1/psbo1-1
psbo1-1
PSI-NDH mc
PSII-LHCII sc
PSI, PSII dimer
ATP synthase
PSII monomer, Cyt b6f
LHCII assembly
LHCII trimer
LHCII monomer
B
Col-0
psbo2-1 PsbO1/psbo1-1
psbo1-1
PSI-LHCI-LHCII
PSI
ATP synthase
PSII monomer, Cyt b6f
LHCII trimer

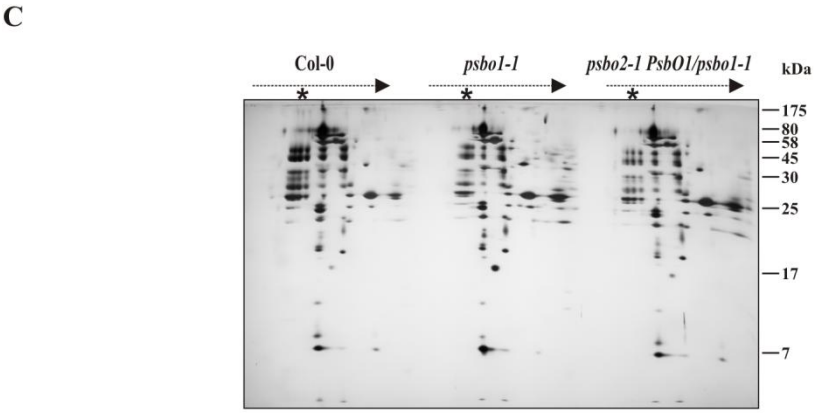
C
Col-0
psbo1-1
psbo2-1 PsbO1/psbo1-1
kDa
175
80
58
45
30
25
17
7

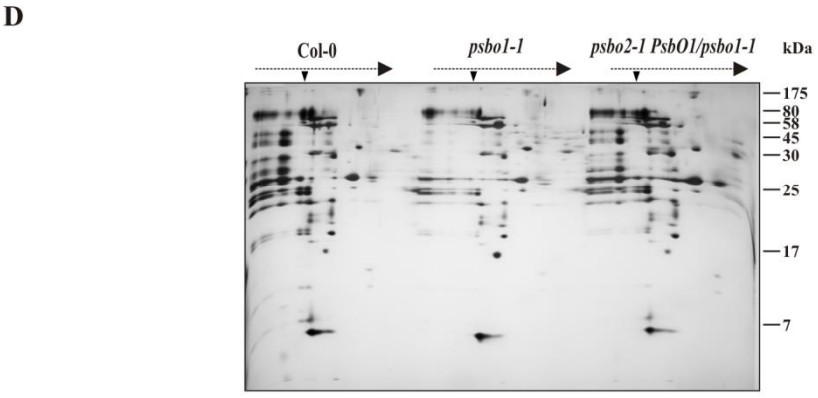
D
Col-0
psbo1-1
psbo2-1 PsbO1/psbo1-1
kDa
175
80
58
45
30
25
17
7

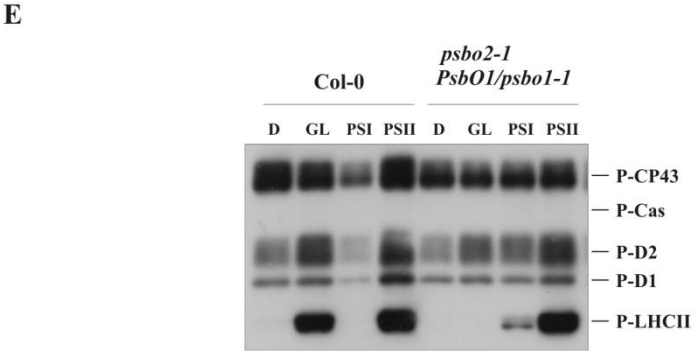
E
Col-0
psbo2-1
PsbO1/psbo1-1
D
GL
PSI
PSII
D
GL
PSI
PSII
P-CP43
P-Cas
P-D2
P-D1
P-LHCII

Figure S3. Blue Native, 2D SDS-PAGE and phosphoblot analyses of thylakoid membrane protein complexes isolated from Col-0 and mutant leaves expressing either PsbO2 protein alone (*psbo1-1*) or a reduced amount of PsbO1 subunit (*psbo2-1 PsbO1/psbo1-1*). (A) Thylakoid membranes isolated from mature Col-0 and mutant plants were solubilised with 1% w/v β-dodecyl maltoside prior to fractionation by large-pore Blue Native PAGE (lpBN-PAGE) (B) Thylakoid membranes isolated from the same set of genotypes were also solubilised with 1.0 % w/v digitonin and fractionated by lpBN-PAGE. (C) The BN gel lanes shown in (A) were subjected to denaturing PAGE, and the 2D gels were stained with silver. (D) The BN gel lanes in (B) were fractionated and stained as in (C). (E) Phosphorylation levels of LHCII (P-LHCII), Cas (P-Cas) and PSII core proteins (P-D1, P-D2 and P-CP43). One of the three immunoblots prepared for each genotype is shown. Thylakoid proteins extracted from leaves of mature Col-0 and *psbo2-1 PsbO1/o1* mutant plants, kept overnight in the dark (D), and subsequently exposed to growth light (GL), PSI-enriched light (PSI) or PSII-enriched light, were fractionated by SDS-PAGE, transferred to PVDF membranes and immunodecorated with a polyclonal anti-phosphothreonine antibody. NDH, NAD(P)H dehydrogenase; PS, photosystems; LHC, light-harvesting complex; Cyt b_6f, cytochrome b_6f; sc, supercomplex; mc, megacomplex.

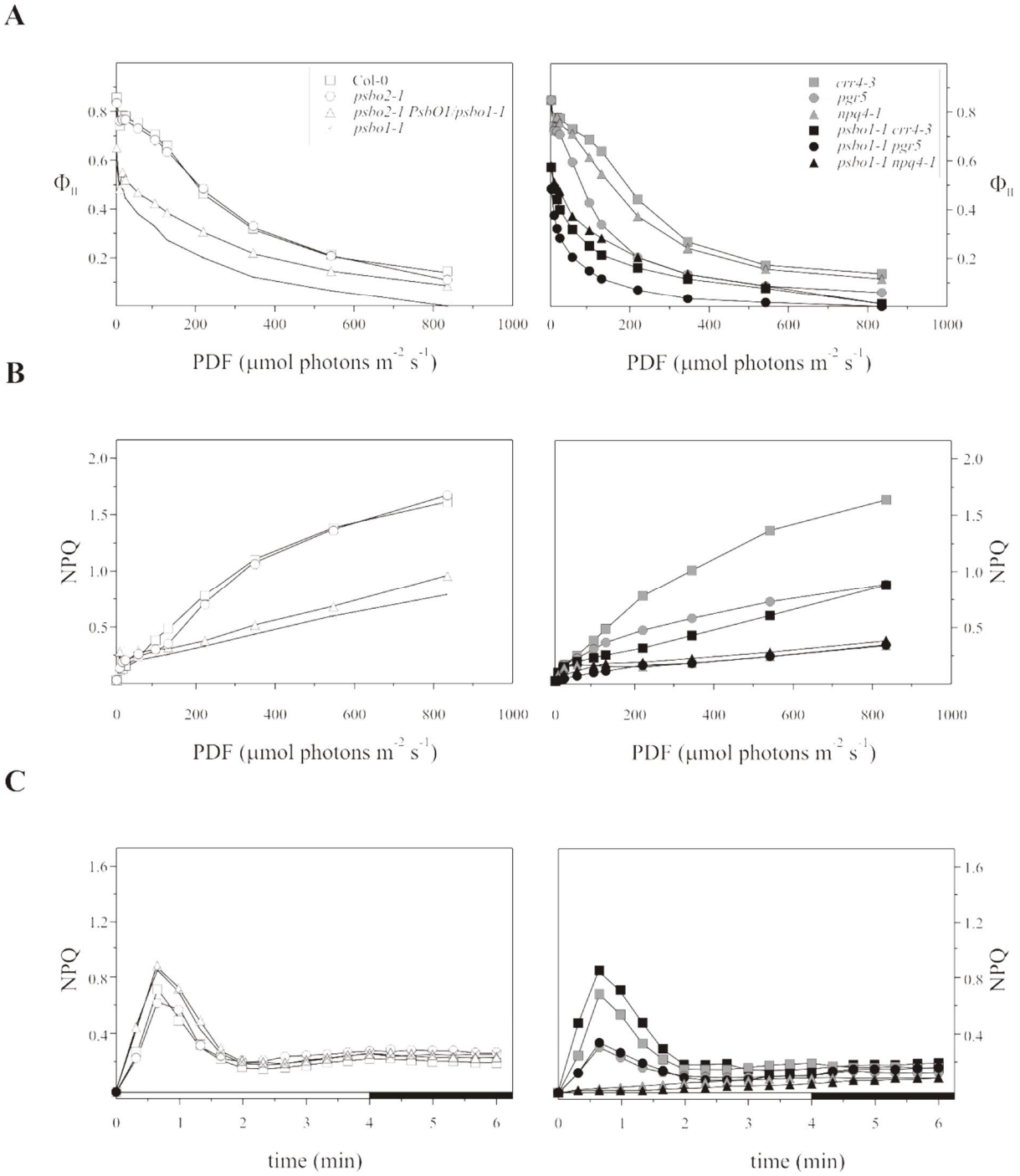

Figure S4. Photosynthetic performance of WT (Col-0) and mutant plants. (A) The photosynthetic parameters F_V/F_M (dark-adapted), Φ_{II} (light adapted) and (B) steady-state NPQ were measured in WT and mutant plants at the 8-leaf rosette stage, grown under low light conditions (80 µmol photons m^{-2} sec^{-1}), dark-adapted for 30 min and illuminated for 2 min with various light intensities. Fluorescence was recorded after dark adaptation and at the end of each illumination period. PDF, photosynthetically active flux density. (C) Time-courses of induction and relaxation of NPQ monitored during the dark-to-light (53 µmol photons m^{-2} sec^{-1}, white bar) transition. The 4-min light period (white bar) was then followed by a 2-min dark period (black bar). Note that NPQ

induction during the activation period of photosynthesis is thought to be caused by the transient acidification of the thylakoid lumen when CET activity exceeds that of the ATP synthase.

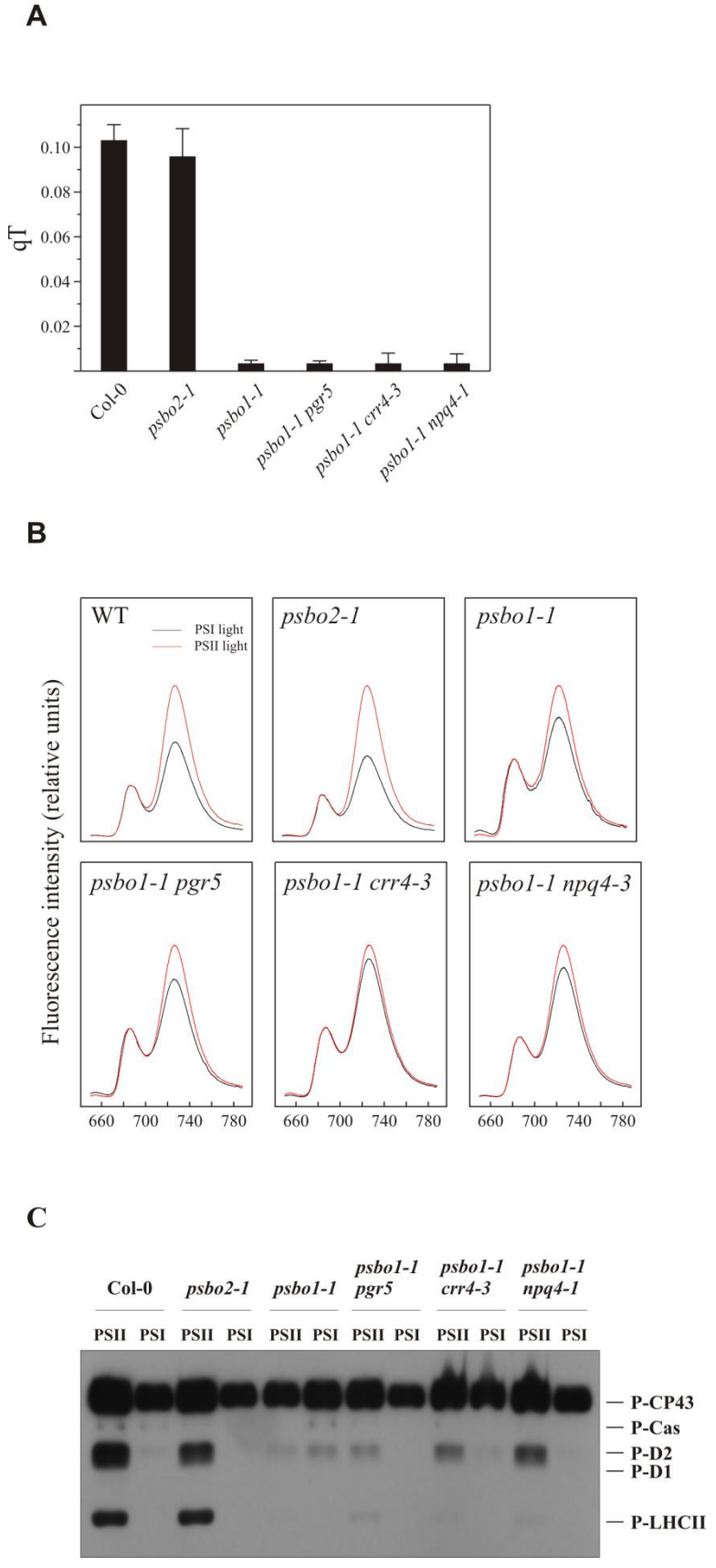

Figure S5. State Transitions in WT (Col-0) and mutant plants. (A) Quenching of chlorophyll fluorescence due to state transitions (qT). Mean values obtained from five independent measurements for each genotype are reported. Bars indicate standard deviations. (B) Low-

temperature (77 K) fluorescence emission spectra of thylakoids after exposure of plants to light inducing either state 1 (black lines, far-red light of 740 nm) or state 2 (red lines, low light; 80 mmol m^{-2} s^{-1}) (see also Methods). The excitation wavelength was 475 nm, and spectra were normalized with reference to peak height at 685 nm. Traces are the average of 5 replicates. (C) Thylakoids as in (B) were fractionated by SDS-PAGE, transferred to PVDF membranes and probed with a polyclonal anti-phosphothreonine antibody. Levels of phosphorylation of LHCII (P-LHCII), Cas (P-Cas) and PSII core proteins (P-D1, P-D2 and P-CP43) detected on one representative immunoblot (n=3) for each genotype are shown.

Table S1. Oligonucleotide sequences employed for genotyping insertion lines. Gene-specific sense (SP) and antisense (ASP) oligonucleotide combinations were used to identify the WT alleles, whereas T-DNA and gene-specific oligonucleotide combinations (either SP or ASP) were employed to detect the mutant alleles. In the case of *CRR4* and *PGR5* loci, the mutant alleles were identified by amplifying a portion of the gene with the corresponding SP and ASP primers and sequencing of the amplicons. For *NPQ4* locus the SP and ASP primer combination was only able to amplify the WT allele

Locus (allele)	Sense primer (SP)	Antisense primer (ASP)	T-DNA specific primer (TSP)	Primer combination
PsbR (psbr)	AGGAATTAACGGCAGCATGG	ACTGAGCCAAAGCACTTGTG	LbB1: GCGTGGACCGCTTGCTGCAACTC	LbB1/ASP
PsbQ1 (psbq1-1)	TCAAAGGTCTAGACTTGTCGTCAGAG	CAAAATCTTGATAGATGGTGATCG	LbB1: GCGTGGACCGCTTGCTGCAACTC	LbB1/SP
PsbQ2 (psbq2-1)	CAGAACGTGTCAGTACCAGAAAGT	ATACTTCTCAGCATCTGGGTCACT	LbB1: GCGTGGACCGCTTGCTGCAACTC	LbB1/ASP
PsbP2 (psbp2-1)	TCGTTTCGTCATGTGTCCCT	CTTGCTTCCCGAGGAGATAA	LbB1: GCGTGGACCGCTTGCTGCAACTC	LbB1/ASP
PsbO1(psbo1-1)	CCTGACTGAGACAGTATCCA	GGAGAGTCGGAGATTAAAGA	Atp3237: TCCGTTCCGTTTTCGTTTTTTAC	Atp3237/ASP
PsbO2(psbo2-1)	AACTATCGATGGTGGCTCTG	GCATTATCGTACCCAGTGGA	LbA1: ATGGTTCACGTAGTGGGCCATC	LbA1/ASP
PsbO2(psbo2-2)	TCAGGGAAACCCGAAAGCTT	ATCACTCAATCTGACCGTAC	LbA1: ATGGTTCACGTAGTGGGCCATC	LbA1/SP
CRR4 (crr4-3)	AGGAGAGTCACTTGTTACCC	TTGGCTCAACAGGCATTTCC		SP/ASP
PGR5 (pgr5)	TCAGAGGAAAAGCCATTGCC	TCAGATGAGAATGGCAGCAG		SP/ASP
NPQ4 (npq4-1)	TCCTTCTCTCATCCTCAGAAA	CAACATGAAGAGAAGGTCAC		SP/ASP